SPATIOTEMPORAL HETEROGENEITY DECOUPLES INFECTION PARAMETERS OF AMPHIBIAN CHYTRIDIOMYCOSIS

Kirsten M. McMillan[1,2], David Lesbarrères[2], Xavier A. Harrison[1,3], & Trenton W. J. Garner[1]

[1] Institute of Zoology, Zoological Society of London, London NW1 4RY, UK.

[2] Department of Biology, Laurentian University, Sudbury, Ontario P3E 2C6, Canada.

[3] University of Exeter, Stocker Road, Exeter EX4 4QD, UK.

Corresponding author:

Kirsten M. McMillan

Dogs Trust, 17 Wakley Street, London EC1V 7RQ

kirsten.marie.mcmillan@gmail.com

Abstract

1. Emerging infectious diseases are responsible for declines in wildlife populations around the globe. Mass mortality events associated with emerging infectious diseases are often associated with high number of infected individuals (prevalence) and high pathogen loads within individuals (intensity). At the landscape scale spatial and temporal variation in environmental conditions can alter the relationship between these infection parameters and blur the overall picture of disease dynamics.
2. Quantitative estimates of how infection parameters covary with environmental heterogeneity at the landscape scale are scarce. Predicting rates of pathogen transmission and identifying wild populations at risk of disease epidemics requires that we elucidate the factors that shape, and potentially decouple, the link between pathogen prevalence and intensity of infection over complex ecological landscapes.
3. Using a network of 41 populations of the amphibian host *Rana pipiens* in Ontario, Canada, we present the spatial and temporal heterogeneity in pathogen prevalence and intensity of infection of the chytrid fungus *Batrachochytrium dendrobatidis* (*Bd)*, across a 3-year period. We then quantify how covariation between both infection parameters measured during late summer, are modified by previously experienced spatiotemporal environmental heterogeneity across 14 repeat sampled populations.
4. Late summer *Bd* infection parameters are governed, at least in part, by different environmental factors operating during separate host life history events. Our results provide evidence for a relationship between *Bd* prevalence and thermal regimes prior to host breeding at the site level, and a relationship between intensity of infection and aquatic conditions (precipitation, hydroshed size and river density) throughout host breeding period at the site level. This demonstrates that

microclimatic variation within temporal windows, can drive divergent patterns of pathogen dynamics within and across years, by effecting changes in host behaviour which interfere with the pathogen's ability to infect and re-infect hosts.

5. A clearer understanding of the role that spatiotemporal heterogeneity has upon infection parameters will provide valuable insights into host-pathogen epidemiology, as well as more fundamental aspects of the ecology and evolution of interspecific interactions.

Keywords: *Batrachochytrium dendrobatidis*, spatiotemporal, environmental heterogeneity, host phenology, prevalence, intensity of infection, mixed-effects model, *Rana pipiens*.

Introduction

Emerging infectious diseases (EIDs) pose a significant threat to the conservation of global biodiversity and are responsible for species declines and extinctions around the globe (Fisher et al., 2012). EIDs are commonly characterized by both efficient pathogen transmission, manifesting as high prevalence, and accumulation of pathogen loads within infected hosts, i.e. high intensity of infection. Though prevalence and intensity of infection may be tightly coupled at the local scale, heterogeneity in both landscape structure and climatic patterns can alter a pathogen's life history and disrupt the association between these two infection parameters at larger spatial scales (Ostfeld et al., 2005). Both infection parameters may independently respond to multiple, interacting, and often nonlinear environmental variables in very different ways (Altizer et al., 2013), meaning complex ecological landscapes may constrain pathogen distribution and the epidemic potential of an infectious disease (Walther et al., 2002). Though it has long been recognized that environmental heterogeneity has the ability to modify the strength of interactions between hosts and pathogens, quantitative estimates of how infection parameters covary with environmental variability at the landscape scale are scarce. If we are to predict rates of pathogen transmission and eventually identify wild populations at risk of epidemics, we must elucidate factors that shape, and potentially decouple, the link between pathogen prevalence and intensity of infection over highly heterogenous ecological landscapes. Using a network of 41 populations of the amphibian host *Rana pipiens (R. pipiens,* Northern Leopard Frog, formerly *Lithobates pipiens;* Yuan et al., 2016) in Ontario, Canada, we present the spatial and temporal heterogeneity in pathogen prevalence and intensity of infection of the chytrid fungus *Batrachochytrium dendrobatidis* (*Bd*; Longcore et al., 1999), across a 3-year period. We then quantify how covariation between both infection parameters measured

during late summer, are modified by previously experienced spatiotemporal environmental heterogeneity across 14 repeat sampled populations.

Bd has contributed to the decline of at least 501 amphibian species over the past half-century, including 90 species that are confirmed or presumed extinct in the wild (Scheele et al., 2019). One of the most striking features of *Bd* is the variability in outcome of infection that has been observed among populations, within a species. For example, the spread of *Bd* in common midwife toad (*Alytes obstetricans*) populations in Europe has led to high rates of mortality and population crashes, while other populations appear to coexist alongside *Bd* with no evidence of disease (Tobler et al., 2012; Bates et al., 2018). As our understanding of the factors that influence *Bd* infection improves, it is becoming increasingly apparent that infection outcome arises from the interaction between the ecology and evolutionary history of the host (e.g. resistance and tolerance; Wilber et al., 2017), the genotype and phenotype of the fungus (e.g. infectivity and virulence; O'Hanlon et al., 2018), and the surrounding abiotic and biotic environment (e.g. environmental heterogeneity and landscape structure; Kärvemo et al., 2018). However, these factors operate across nested levels of biological organization: within-host processes underlie among-host processes within a population. Consequently, studies looking to gain insight into epidemiological processes of *Bd* must consider within-host up through population-level dynamics. Assessing environmental drivers of *Bd* disease dynamics at this scale is particularly challenging with regards to amphibian hosts, as small-scale spatial heterogeneity contributes towards the physiology of both host and pathogen. As climate acts as a proximate driver for amphibian phenology and daily activity, local climatic nuances will directly influence host activity patterns such as emergence from over-wintering habitat and onset of breeding season (Klaus & Lougheed, 2013). These small-scale spatiotemporal

86 variations may alter the local disease ecology (i.e. prevalence and intensity of infection)
87 by facilitating or compressing opportunities for pathogen transmission and/or growth
88 (Daversa et al., 2017, 2018). Beyond climatic patterns, anthropogenic habitat
89 disturbance may cause a cascade of factors that exacerbate infectious disease
90 emergence. Landscape fragmentation may alter host-pathogen dynamics by regulating
91 host species isolation, inbreeding, and richness (Lesbarrères et al., 2006; Greer &
92 Collins, 2008). Thus, the nature and intensity of an amphibian-parasite interaction will
93 be contingent upon the spatiotemporal patterns of both host and parasite (Hess et al.,
94 2001). Despite this fact, most studies attempting to elucidate environmental drivers of
95 *Bd* disease dynamics have focused on the spatial aspects of environmental
96 heterogeneity alone, overlooking the importance of temporal variation (Pounds et al.,
97 2006; Olson et al., 2013; Xie et al., 2016; however, see Clare et al., 2016). A clearer
98 understanding of the links between environmental parameters, host breeding
99 phenology, and the outcomes of ectothermic host-pathogen interactions will provide
100 valuable insights into host-pathogen epidemiology, as well as more fundamental
101 aspects of the ecology and evolution of interspecific interactions (Lambrechts et al.,
102 2006).

103 Despite the presence of *Bd* within Ontario, Canada (St-Amour et al., 2008;
104 D'Aoust-Messier et al., 2015), chytridiomycosis-driven declines are yet to be
105 definitively reported within populations of *R. pipiens*. Yet, outside of Ontario,
106 chytridiomycosis has been reported as the cause of mass mortality events within this
107 species (Green et al., 2002; Voordouw et al., 2010). Consequently, Ontario populations
108 of *R. pipiens* provide an opportunity to quantify the effect that small-scale
109 environmental variation has on *Bd* infection parameters, in the absence of disease. We
110 assessed adult *R. pipiens* for *Bd* infection status and quantified how prevalence (%) and

intensity of infection (genomic equivalents; GE) covaried with the following site level factors: air temperature, precipitation, hydroshed size, river density, and road density.

In order to measure environmental variation at a scale relevant to the host, temperature and precipitation were averaged across two specific time points: (1) period prior to host breeding, and (2) during host breeding. Based on *a priori* hypotheses regarding the effects of environmental factors on *Bd* disease dynamics, we hypothesize that: (i) during the active period, cooler temperatures and greater precipitation will be associated with increased prevalence and infection intensity in late summer (Piotrowski et al., 2004; Bosch et al., 2007; Puschendorf et al., 2009), due to increased opportunities for successful *Bd* transmission (Lampo et al., 2006); (ii) during the breeding period, as water basins and rivers serve as likely vectors for the waterborne zoospores (Kriger & Hero, 2007), an increase in basin size will lower intensity due to diluted zoospore concentrations (Briggs et al., 2010), while a reduction in river density will limit transmission nodes, thus lowering prevalence and infection intensity (Sapsford et al., 2013; Ruggeri et al., 2018); and (iii) increased road density will intensify landscape fragmentation leading to isolated habitat patches and dense host populations, which will allow for an increase in overall prevalence and intensity (Greer & Collins, 2008; Balkenhol & Waits, 2009).

Materials and Methods

Sampling for *Bd*

Site selection was based on the known whereabouts of *R. pipiens* populations (Fig. S1, Supporting information). Sites were defined as a distinct body of water, where the amphibian population was captured within a 2 km radius from the site centroid. All site centroids were separated by a minimum of 12 km. In total, 41 populations of *R. pipiens* were surveyed for *Bd* (Fig. 1). At each site, up to 34 post-metamorphic frogs were

136 sampled (range: 1-34, mean: 25.6; Table S1, Supporting information). In localities
137 where *R. pipiens* were rare (n < 24), the population was sampled for 30 person-hours.
138 Each study site was geo-referenced using GPS and sampled at least once during the
139 summer months (May-August) of 2012-2014. Within the 41 sites, 14 sites were
140 identified and repeat sampled annually, during the late summer months (July-August)
141 between 2012-2014. Two of the 14 sites were sampled twice within this period, the
142 remaining 12 sites were sampled for three consecutive years. Twenty-four or more post-
143 metamorphic frogs were sampled at the repeat sites (range: 24-34, mean: 30.7; Table
144 S1, Supporting information). Within-site sampling occurred within a 3 week period. To
145 detect infections, we collected a toe-clip from each frog: 2-3 mm clip was cut from the
146 longest front toe on the left hand using sterile dissecting scissors. Toe clipping
147 facilitated identification of previously sampled individuals in subsequent years,
148 consequently no individuals were repeat sampled. Tissue samples were stored in 70%
149 ethanol at 4°C until processing (Hyatt et al., 2007). Standardized protocols and
150 biosecurity measures were followed to prevent pathogen transmission (Phillott et al.,
151 2010). Snout-vent length (SVL) was measured to the nearest 0.01 mm. We
152 distinguished between three life history stages: recent metamorphs (SVL < 45 mm),
153 juveniles (SVL: 45-52 mm) and adults (SVL > 52 mm; Wright & Wright, 1949). When
154 modelling the effect of spatiotemporal environmental heterogeneity on late summer
155 infection parameters, we excluded metamorphs from the analysis as natal dispersal and
156 behaviour is dissimilar to that observed in juveniles and adults (Dole, 1965). DNA was
157 extracted using DNeasy Blood and Tissue kit (Qiagen) according to the manufacturer's
158 instructions. Presence/absence and quantity of *Bd* was then assessed using the
159 quantitative PCR (qPCR) protocol described by Boyle et al. (2004). To avoid inhibition,
160 all extractions were diluted 1/10 prior to qPCR, therefore results were multiplied by 10

161 in order to determine the true value. All samples were run in duplicate, and a sample
162 was considered *Bd* positive if both wells amplified and an average estimate of 0.1 GE
163 or above was produced when comparing the sample to the curve generated by the
164 standards (1000, 100, 1 and 0.1).

165 **Acquisition of environmental data with respect to host life history**

166 The emergence of *R. pipiens* from overwintering sites is triggered by the onset of
167 spring, specifically the first day on which the mean daytime temperature exceeded zero
168 degrees Celsius for fourteen consecutive days. Frogs then become terrestrially active,
169 travelling up to 1.6 km to their breeding ponds (Kendell, 2003). Breeding period
170 commences when male frogs start calling. This occurs when the daytime air
171 temperature persistently averages 15ºC (Seburn, 1992). Both sexes exhibit strong site
172 fidelity and limited movement during the breeding period (Waye & Cooper, 2000). As
173 far as we are aware, there are no quantitative estimates regarding the end of the breeding
174 period for *R. pipiens* within Ontario. Consequently, based on *a priori* knowledge
175 regarding breeding periods for *R. pipiens* across Canada, we subjectively defined the
176 end of the breeding period as the last day of June (Harding, 1997; Stebbins, 2003;
177 Government of Canada, 2009; Voordouw et al., 2010). For the purposes of this study,
178 the period between spring emergence and calling will henceforth be referred to as the
179 '*active period*', and the period between calling and the end of the breeding period will
180 henceforth be referred to as the *'breeding period'*. As these two periods are
181 differentiated by host phenology and local climatic nuances, we wished to record spatial
182 heterogeneities during the two-time periods. Consequently, we collected data on the
183 following: length of active period, air temperature during active period and breeding
184 period, precipitation during active period and breeding period, hydroshed area, river
185 density and road density.

186 Mean daily air temperature (˚C) was compiled from data loggers (HOBO U23
187 Pro v2 Data Logger (U23-001)) activated at 10 sites and weather stations in close
188 proximity to 22 sites (Fig. 1 and Table S1, Supporting information). Any gaps in the
189 hourly records were replaced with data from the second closest weather station (range:
190 1.4-44.69 km, mean: 17.4 km; Government of Canada, 2015a). This dataset allowed
191 for the estimation of the following annual variables: '*spring onset'*, '*calling date*',
192 '*active period*': period between spring onset and calling date; and '*breeding period*':
193 period between the calling date and the last day of June. Each site locality was assigned
194 to a drainage basin, downloaded from USGS HydroSHEDS (Lehner et al., 2008). Mean
195 monthly precipitation was obtained as environmental layers downloaded from the
196 WorldClim data set (version 1.4; Hijmans et al., 2005). Both variables were re-
197 projected and re-sampled to the same equal area grid as the site localities. Hydroshed
198 area (km^2) and mean monthly precipitation (mm) during both the *'active period'* and
199 *'breeding period'* were obtained by extracting the raw value of each variable at all site
200 localities from their raster source. Temperature and precipitation data for 9 sites were
201 not compiled, as only 2% of total individuals were located within these sites (Table S1,
202 Supporting information).
203 River and road cartographic boundary files were obtained from the Statistics
204 Canada census (Statistics Canada, 2011) and the National Road Network for Ontario
205 Geobase (Government of Canada, 2015b), respectively. The density of rivers and roads
206 surrounding each site locality was obtained by calculating the extent to which each
207 spatial line dataframe overlapped a cell within a spatially explicit blank raster, and
208 subsequently extracting the mean value of all raster cells found in a radius of 10 km
209 and 50 km around each site locality, respectively. The apportioned radius for
210 calculating road density was increased from 10 km to 50 km, in order to include

maximum variation recorded in the dataset, with regards to habitat fragmentation and local disturbance. Details regarding the variations (per grid cell), raw resolutions, year of record, unit and source for all spatial predictors are listed in Table S2 (Supporting information).

Statistical analyses

All statistical analyses were implemented in R (version 3.1.2; R Core Team, 2015). Linear regression was carried out to assess the relationship between length of active period (days), spring onset (decimal date), calling date (decimal date), and year. Presence of infection was compared between sites using a Fisher's exact test for count data. Variation in prevalence and infection intensity (rounded to whole numbers and treated as count data) were compared between sites, years, and development status (adult/juvenile) with χ^2 tests and univariate ANOVA, respectively. Any significant results from ANOVA testing were further tested using Tukey *post hoc* tests in order to determine which categorical groupings were different from the others. We included data from all 41 sites in the above tests in order to increase precision of estimates. However, in order to disentangle spatial from temporal effects over the 3 year period, the following modelling exercise was restricted to 14 sites visited at least twice, during the late summer months (July-August) between 2012-2014 inclusive, with at least 24 frogs sampled per year (Fig. 1 and Table S1, Supporting information). Two separate generalized linear mixed models (GLMMs) were constructed, implementing a Binomial error structure for the *Bd* prevalence model and a Negative Binomial error structure to the *Bd* intensity of infection model (mean GE). We accounted for possible non-independence of samples collected at the same site locality by including a random intercept effect for site ID (n=14) and added year as a fixed effect. We did not expect serial autocorrelation to be present in the data as sampling occurred once per year.

Excluding all models that included confounding pairs of covariates (absolute correlation coefficient > 0.5), we constructed a set of 31 competing candidate models to test against *Bd* prevalence (Table S3, Supporting information) and *Bd* intensity of infection, separately (Table S4, Supporting information). Predictor variables included: length of active period (days), mean daily air temperature (˚C) throughout active period, mean daily air temperature (˚C) throughout breeding period, mean precipitation (mm) throughout active period, mean precipitation (mm) throughout breeding period, hydroshed area (km^2), river density (within 10 km buffer from site centroid) and road density (within 50 km buffer from site centroid). All variables were z-transformed [(x-mean)/SD] prior to analysis to have a mean of 0 and standard deviation of 1, putting all predictors on a common scale, and making main effects interpretable in the presence of interactions. We used an information-theoretic approach to identify the model(s) with the strongest support in the data. Specifically, we used Akaike's information criterion (AIC) to select among the intensity of infection models, and quasi-AIC (QAIC) for *Bd* prevalence models in order to correct for overdispersion (c-hat=6.45; Burnham & Anderson, 2002). We used a delta-6 information criterion cut off for the top model set, where all models within 6 points of the model with the best support in the data (lowest IC score) were considered to have roughly equivalent support (Harrison et al., 2018). Furthermore, we applied the 'nesting rule', in which models that are more complex versions of models with better support (lower AIC) are removed from the top model set (Richards et al., 2011; Harrison et al., 2018). Remaining models were selected for model averaging. We present model-averaged predictions from these models alongside predictions from the top model. Predicted means and 95% credible intervals were extracted based on 1000 simulations (Gelman & Hill, 2007).

Results

We collected 2223 toe clips from post-metamorphic *R. pipiens*, captured from 41 sites in Ontario. Of the 2223 *R. pipiens* sampled, 833 were sampled in 2012, 878 were sampled in 2013, and 512 were sampled in 2014. Overall prevalence was 28.9%. Infection was detected across a broad geographic range (36 of 41 sites were infected; Fig. 1) and despite presence of strong infections (maximum GE = 7427.23, Table S1, Supporting information) no mortality or moribund individuals were observed. We sampled 1229 *R. pipiens* within the 14 repeat sampled sites; 75% of individuals were sampled post breeding period, while the remaining 25% were sampled within 10 days of the final day of the breeding period.

Bd prevalence (%) and intensity of infection (GE) did not vary between adults and juveniles. However, both infection metrics varied significantly between years. Prevalence in 2013 was significantly higher than 2012 and 2014 ($\chi^2 = 69.7$, $p < 0.0001$, df = 1; $\chi^2 = 149.2$, $p < 0.0001$, df = 1, respectively). We recorded a 79.8% increase in prevalence between 2012 and 2013, and a 73.1% decrease in prevalence between 2013 and 2014 (Fig. S2, Supporting information). Infection intensity (GE) was also greatest in 2013 (mean GE [SE] = 138.8 [19.1], maximum GE = 7427.2, $F_{2, 2220} = 32.8$, $p < 0.0001$) than 2012 (mean GE [SE] = 16.9 [4.4], maximum GE = 2708.3; $p < 0.0001$) or 2014 (mean GE [SE] = 2.7 [0.8], maximum GE = 312.3; $p < 0.0001$; Fig. S3, Supporting information). Sites repeat sampled in 2012 and 2013 showed variation in prevalence ($\chi^2 = 255.2$, $p < 0.001$, df = 13; $\chi^2 = 165.3$, $p < 0.001$, df = 13, respectively) and infection intensity ($F_{33, 799} = 2.7$, $p < 0.001$; $F_{33, 842} = 7.3$, $p < 0.0001$). However, neither prevalence nor intensity varied between sites in 2014, as both infection measures remain consistently low (Fig. 2).

Frogs experienced cooler temperatures during their active period in 2013 in comparison to 2012 ($F_{1, 77} = 7.9$, $p < 0.01$), but no other among-year comparisons were

significant (Table 1). Frogs also experienced cooler temperatures during their breeding period in 2013 in comparison to 2012 ($F_{1, 77} = 8.4$, $p < 0.01$) and 2014 ($F_{1, 77} = 26.9$, $p < 0.0001$; Table 1). Mean precipitation throughout the active or breeding period did not differ between years (Table 1). Decimal date for both spring onset and calling date differed significantly between years ($F_{4, 160} = 50.0$, $p < 0.0001$; $F_{4, 160} = 14.1$, $p < 0.0001$, respectively) with 2012 exhibiting earlier dates than any other year (Table 2).

There was a shift towards a later spring date, with an average delay of 0.21 days per annum ($t = 3.79$, $p < 0.001$; Table 3), and an earlier calling date, with the advancement of 5.13 days per annum ($t = -2.45$, $p < 0.05$; Table 3). Despite observing a 27.85 day delay between the 2012 and 2013 spring onset, the 2013 calling date was delayed by a mere 3.97 days. Correspondingly, the length of active period differed significantly between years ($F_{4, 160} = 15.9$, $p < 0.0001$) with 2013 exhibiting a shorter active period than all other years. On average, there was a shift towards a shorter active period, with an average reduction of 5.33 days per annum ($t = -4.89$, $p < 0.001$; Table 3).

Factors predicting *Bd* prevalence in late summer

Restricting the model to the 14 repeat sampled sites, the model predicting *Bd* prevalence, with the highest support in the data, comprised of an interaction between mean daily air temperature during active period and length of active period. After applying the nesting rule, there were four models in the delta-6 QAIC candidate set (Table S3, Supporting information, see Table 4 for model-averaged estimates). *Bd* prevalence was negatively correlated with mean daily air temperature during active period, while prevalence increased as the length of active period was extended (Fig. 3). More specifically, as length of active period increased, the negative relationship between *Bd* prevalence and mean daily air temperature weakened, while the variation

311 in *Bd* prevalence remained relatively constant throughout the range of temperatures.
312 Conversely, as length of active period shortened, the negative effect of mean daily air
313 temperature on *Bd* prevalence strengthened (larger negative slope), while variation in
314 *Bd* prevelance fluctuated dependent on temperature. The highest prevalence outcome
315 was predicted to occur when the active period was shortened and when mean air
316 temperature was coolest.

317 **Factors predicting *Bd* intensity in late summer**

318 Models predicting intensity of infection, were generated using the 14 repeat sampled
319 sites. There were three models in the delta-6 AIC candidate set after applying the
320 nesting rule (Table S4, Supporting information, see Table 4 for model-averaged
321 estimates). The best-supported model included hydroshed area, and an interaction
322 between river density and mean precipitation throughout breeding period. Intensity of
323 infection (mean GE) was negatively correlated with hydroshed area (Fig. 4), but
324 positively correlated with both river density and mean precipitation throughout
325 breeding period (Fig. 5). As river density increased, the positive relationship between
326 infection intensity and mean precipitation during breeding period became significantly
327 stronger (larger positive slope). As both predictor variables increased, infection
328 intensity grew exponentially. Within site localites with low surrounding river densites,
329 mean infection intensity only increased when precipitation levels were low.

330 **Discussion**

331 Our results highlight that spatial variation in pathogen prevalence and infection
332 intensity at the landscape scale is driven by the covariation between host behaviour and
333 local environmental conditions. Within sites, strong prevalence and intensity of *Bd*
334 infection in late summer emerged when previous temperatures were low, rainfall was

335 high, hydrosheds were small, and river networks were dense. This suggests that
336 interannual variation of local climatic regimes interact with stable geographic factors
337 (such as hydrology), to inhibit the build-up of *Bd* infection intensity and prevalence.
338 More specifically, our analyses show evidence for: (1) the existence of both spatial and
339 temporal heterogeneity in infection among sites; (2) evidence for a relationship between
340 *Bd* prevalence and thermal regimes prior to host breeding at the site level; (3) evidence
341 for a relationship between infection intensity and aquatic conditions throughout host
342 breeding period at the site level; and (4) no evidence for a relationship between *Bd*
343 prevalence/ infection intensity, and road density. Furthermore, despite the fact that
344 studies may predict implicit deterministic relationships between *Bd* prevalence and
345 infection intensity, these infection parameters are governed, at least in part, by different
346 environmental factors operating during separate life history events. This emphasizes
347 the importance of measuring both infection parameters within a spatiotemporal context,
348 when attempting to gain insight into *Bd* infection dynamics.

349 Once *R. pipiens* emerge from their overwintering sites, local climatic conditions
350 may determine whether *Bd* is able to establish within a population. Localities that
351 experienced short warm climates prior to breeding were unlikely to support the
352 establishment of *Bd,* while sites that experienced cold temperatures, irrespective of
353 duration, were most likely to harbour *Bd* infections in late summer. These results
354 support both bioclimatic predictive models (Ron, 2005; Puschendorf et al., 2009) and
355 laboratory studies (Longcore et al., 1999; Johnson et al., 2003) that point to *Bd* being
356 favoured by cooler temperatures. However, the temperatures experienced during the
357 active period are well below lab-based estimates of the optimal thermal range for fungal
358 growth (17-25°C; Longcore et al., 1999; Johnson et al., 2003). Woodhams et al. (2008)
359 identified that at lower temperatures growth rate slows, but fecundity and the life span

360 of the zoospore increase, which should influence probability of infection. This is
361 consistent with our observations of higher prevalence in populations experiencing
362 cooler climates.

363 Our climate analyses provide evidence for the shortening of active period by
364 5.33 days per annum or 21.33 days over the four-year period. As *Bd* prevalence is
365 predicted to decrease as the length of active period decreases, it would seem reasonable
366 to suggest this annual curtailment may lower the infection risk faced by *R. pipiens*
367 populations. Conversely, 2013 presented the shortest active period and the highest *Bd*
368 prevalence. Frogs sampled in 2013 also experienced the coolest mean temperatures
369 during the active period. This highlights the importance of the interaction between the
370 two variables. The extension or shortening of the active period has little effect on *Bd*
371 prevalence when mean temperatures are low (between 5-8°C). Extending this period
372 when temperatures are warm (10-12°C), generates an increase in prevalence, while
373 limiting this period leads to a reduction in prevalence. We suggest that this pattern may
374 be due to expanded opportunities for the successful transmission of *Bd* between
375 individuals when the active period is elongated and warmer.

376 All variables that correlate with *Bd* mean intensity are emergent properties of
377 site hydrology: hydroshed area, surrounding river density, and mean precipitation
378 throughout the breeding period. This corroborates predictions that *Bd* should be more
379 abundant in wetter areas (Ron, 2005; Kriger et al., 2007), and field studies indicating
380 that *Bd* outbreaks might be more likely under wet conditions (Lips et al., 2006; Bosch
381 et al., 2007). Yet, no published study has linked infection intensity with a reduction in
382 either (1) the size of water basin (hydroshed area), or (2) the density of river networks
383 (however, see Spitzen-van der Sluijs et al., 2017; Kärvemo et al., 2018). We found that
384 as hydroshed area increased, infection intensity decreased slightly, suggesting that *R.*

385 *pipiens* populations concentrated within a small drainage basin may facilitate the
386 proliferation and transmission of zoospores, as increasing host population density
387 increases transmission rates (Briggs et al., 2010). Additionally, larger hydrosheds may
388 allow for greater dilution of zoospores, and thus the frequency with which a zoospore
389 interacts with a host may decrease with increasing spatial context. However, the
390 predicted effect of hydroshed area on mean *Bd* intensity (predicted *Bd* mean intensity
391 range: 0-20 GE) is significantly weaker than the predicted effect of the complex
392 interaction (river density and mean precipitation) on mean *Bd* intensity (predicted *Bd*
393 mean intensity range: 0-500 GE). Mean infection intensity is predicted to increase
394 exponentially when precipitation levels during the breeding period are high, and when
395 frogs are located at sites containing dense river concentrations. When precipitation
396 levels are low during the breeding period, high river density sites will elicit no variation
397 from the global mean, while sites surrounded by very few rivers will experience a small
398 increase in mean infection intensity. There are two hypotheses that can explain these
399 patterns. First, rivers serve as likely vectors for the waterborne zoospores of *Bd* (Kriger
400 & Hero, 2007). A high concentration of rivers within a 10 km^2 area suggests an increase
401 in transmission channels via aquatic nodes, or feasible amphibian movement between
402 catchments. The connectivity of river networks may prove particularly influential as
403 zoospores may be carried away with water currents, thus expanding the spatial reach of
404 infection. When precipitation levels are high, moisture levels will be elevated within
405 the terrestrial environment, along with the aquatic, which increase zoospore movement,
406 survival and colonization (Piotrowski et al., 2004). This is especially important for this
407 host-pathogen interaction, as *R. pipiens* is a semi-terrestrial anuran. Consequently,
408 when individuals are active within the terrestrial realm, increased moisture from heavy
409 rainfall facilitates reinfection from zoospores released within the skin and onto the skin

surface, in turn aiding the significant increase in infection intensity (Daversa et al., 2018). Alternatively, weak precipitation levels lead to dryer environments, especially when rivers are not well connected. This may force individuals to congregate in smaller pools, thus increasing opportunity for successful *Bd* transmission. However, zoospore growth will also be constrained during this period, due to limited moisture availability within the terrestrial realm (Johnson et al., 2003, Daversa et al., 2018). The shared theme in these two hypotheses is the role of re-infection. We suggest that the increase in strength of infection in the system is largely attributable to within-host reinfection (from zoospores released within the skin and onto the skin surface) rather than among-host transmission.

Akin to other ectotherms, the health of amphibians is sensitive to changes in ambient temperatures (Raffel et al., 2006). Despite this, the role of climate change in the unprecedented decline of ectothermic biodiversity and emergence of infectious diseases remains controversial (Rohr et al., 2011). Impacts of climate change on host-pathogen dynamics are expected to be particularly strong for ectotherms, as host metabolism and activity patterns are closely linked to environmental temperatures, which in turn, directly influence the establishment of the pathogen. Less attention has been devoted to the consequences of changes in precipitation and water availability. A strong impact is expected for host and pathogen, as both species rely on humid environments, require water for reproduction, and are particularly active during wet periods. It is imperative that we trace activity patterns and assess the environment in which these infection dynamics operate, as the value of predictive modelling for infection risk increases substantially when parameters affecting local host species-specific infection dynamics are considered at a local scale (Paaijmans et al., 2009). However, with the current absence of quantitative summaries across multiple studies,

it is difficult to identify general patterns. These results of differential, context-dependent host susceptibility to *Bd* is supported by Doddington et al., (2013) and may be a pattern exhibited by other fungal pathogens that threaten wildlife hosts (Fisher et al., 2012). This observation highlights a crucial need for long-term ecological studies that examine the consequences of climate-disease interactions within local communities, as changing environmental conditions could shift the balance from co-existence to significant mortality in some populations, but not in others. This knowledge will directly affect the framing and development of conservation efforts to mitigate infections. Furthermore, studying the patterns of local infections may be crucial to understanding how infection dynamics affect biodiversity at larger spatial scales. Hence, we stress the exigency to identify how local factors may exacerbate or reduce the impact of an infectious disease.

Acknowledgments

We would like to thank A. M. D'Aoust-Messier, B. Grainger-Wood, A. Colles, S. S. Cruickshank and B. J. Varela for assisting with field work and logistics. Field surveys and specimen collection were conducted under the Ontario Ministry of Natural Resources Wildlife Scientific Collector's Authorization (#1068178). Amphibian sampling within protected areas followed permit guidelines awarded by: Parks Canada Agency (#BPF-2013-13913); Ontario Ministry of Natural Resources and Forestry (#4534); Nature Conservancy of Canada (#AG-ON-2012-144055); and St. Clair Region Conservation Authority (#SCRCA-2012-28-05). TWJG and KMM were supported by NERC (NE/G002193/1) and KMM by the Ontario Trillium Scholarship.

Authors' contributions

KMM conceived the ideas and designed methodology; KMM collected the data; KMM and XAH analysed the data; KMM led the writing of the manuscript. All authors contributed critically to the drafts and gave final approval for publication.

Data availability

Data are available from the Figshare repository: https://figshare.com/account/home#/projects/71426 (McMillan et al., 2019).

References

Altizer, S., Otsfeld, R. S., Johnson, P. T., Kutz, S., & Harvell, C. D. (2013). Climate change and infectious diseases: from evidence to a predictive framework. Science, 341(6145), 514-519. doi: 10.1126/science.1239401

Balkenhol, N., & Waits, L. P. (2009). Molecular road ecology: exploring the potential of genetics for investigating transportation impacts on wildlife. Molecular Ecology, 18(20), 4151-4164. doi: 10.1111/j.1365-294X.2009.04322.x

Bates, K. A., Clare, F. C., O'Hanlon, S., Bosch, J., Brookes, L., Hopkins, K., … Harrison, X. A. (2018). Amphibian chytridiomycosis outbreak dynamics are linked with host skin bacterial community structure. Nature Communications, 9(693). doi: 10.1038/s41467-018-02967-w

Bosch, J., Carrascal, L. M., Duran, L., Walker, S., & Fisher, M. C. (2007). Climate change and outbreaks of amphibian chytridiomycosis in a montane area of Central Spain; is there a link? Proceedings of the Royal Society B: Biological Sciences, 274(1607), 253-260. doi: 10.1098/rspb.2006.3713

Boyle, D. G., Boyle, D. B., Olsen, V., Morgan, J. A. T., & Hyatt, A. D. (2004). Rapid quantitative detection of chytridiomycosis (*Batrachochytrium dendrobatidis*) in amphibian samples using real-time Taqman PCR assay. Diseases of Aquatic Organisms, 60(2), 141-148. doi: 10.3354/dao060141

Briggs, C. J., Knapp, R. A., & Vredenburg, V. T. (2010). Enzootic and epizootic dynamics of the chytrid fungus pathogen of amphibians. Proceedings of the National Academy of Sciences of the USA, 107(21), 9695-9700. doi: 10.1073/pnas.0912886107

Burnham, K. P., & Anderson, D. R. (2002). Model selection and multimodel inference: a practical information-theoretic approach (2nd ed.). Springer-Verlag, New York.

488 Clare, F. C., Halder, J. B., Daniel, O., Bielby, J., Semenov, M. A., Jombart, T.,
489 …Fisher, M. C. (2016). Climate forcing of an emerging pathogenic fungus across a
490 montane multi-host community. Philosophical Transactions of the Royal Society,
491 B371, 20150454. doi:10.1098/rstb.2015.0454

492 D'Aoust-Messier, A. M., Echaubard, P., Billy, V., & Lesbarrères, D. (2015).
493 Amphibian pathogens at northern latitudes: presence of chytrid fungus and ranavirus in
494 northeastern Canada. Diseases of Aquatic Organisms, 113(2), 149-155. doi:
495 10.3354/dao02837

496 Daversa, D. R., Manica, A., Bosch, J., Jolles, W. J., & Garner, T.W.J. (2018). Routine
497 habitat switching alters the likelihood and persistence of infection with a pathogenic
498 parasite. Functional Ecology, 32(5), 1262-1270. doi: 10.17863/CAM.20593

499 Daversa, D. R., Fenton, A., Dell, A. I., Garner, T.W.J., & Manica, A. (2017). Infections
500 on the move: how transient phases of host movement influence disease spread.
501 Proceedings of the Royal Society of London. Series B: Biological Sciences, 284(1869),
502 20171807. doi: 10.1098/rspb.2017.1807

503 Doddington, B. J., Bosch, J., Oliver, J. A., Grassly, N. C., Garcia, G., Schmidt, B. R.,
504 … Fisher, M. C. (2013). Context-dependent amphibian host population response to an
505 invading pathogen. Ecology, 94(8), 1795-1804. doi: 10.1890/12-1270.1

506 Dole, J. W. (1965). Spatial relations in natural populations of the leopard frog, *Rana*
507 *pipiens* Schreber, in northern Michigan. American Midland Naturalist, 74(2), 464-478.
508 doi: 10.2307/2423276

509 Fisher, M. C., Henk, D. A., Briggs, C. J., Brownstein, J. S., Madoff, L. C., McCraw, S.
510 L., & Gurr, S. J. (2012). Emerging fungal threats to animal, plant and ecosystem health.
511 Nature, 484(7393), 186-194. doi: 10.1038/nature10947

512 Gelman, A., & Hill, J. (2007). Data analysis using regression and multilevel/
513 hierarchical models. Cambridge University Press.

514 Government of Canada (2015a). Historical Data. Available:
515 http://climate.weather.gc.ca/historical_data/search_historic_data_e.html [accessed:
516 2015 June 10].

517 Government of Canada (2015b). National Road Network (NRN) - Ontario. Available:
518 https://open.canada.ca/data/en/dataset/3d282116-e556-400c-9306-ca1a3cada77f
519 [accessed: 2015 June 10].

520 Government of Canada (2009). Species Profile: Northern Leopard Frog Western
521 Boreal/Prairie populations. Available: https://wildlife-species.canada.ca/species-risk-
522 registry/species/speciesDetails_e.cfm?sid=552 [accessed 2013 January 12].

523 Green, D. E., Converse, K. A., & Schrader, A. K. (2002). Epizootiology of sixty-four
524 amphibian mortality and morbidity events in the USA, 1996 - 2001. Annals of the New
525 York Academy of Sciences, 969(1), 323-339. doi: 10.1111/j.1749-
526 6632.2002.tb04400.x

527 Greer, A. L., & Collins, J. P. (2008). Habitat fragmentation as a result of biotic and
528 abiotic factors controls pathogen transmission throughout a host population. Journal of
529 Animal Ecology, 77(2), 364-369. doi: 10.1111/j.1365-2656.2007.01330.x

530 Harding, J. H. (1997). Amphibians and reptiles of the Great Lakes Region. University
531 of Michigan Press, Ann Arbor, Michigan, USA.

532 Harrison, X. A., Donaldson, L., Correa-Cano, M. E., Evans, J., Fisher, D. N., Goodwin,
533 C., … Inger, R. (2018). A brief introduction to mixed effects modelling and multi-
534 model inference in ecology. PeerJ, 6, e4794. doi:10.7717/peerj.4794

Hess, G. R., Randolph, S. E., Arneberg, P., Chemini, C., Furlanello, C., Harwood, J., … Swinton, J. (2001). Spatial aspects of disease dynamics. In P. J. Hudson, A. Rizzoli, B. T. Grenfell, H. Heesterbeek & A. P. Dobson (Eds.), The ecology of wildlife diseases (pp. 102-118). Oxford, UK: Oxford University Press.

Hijmans, R. J., Cameron, S. E., Parra, J. L., Jones, P. G., & Jarvis, A. (2005). Very high resolution interpolated climate surfaces for global land areas. International Journal of Climatology, 25(15), 1965-1978. doi: 10.1002/joc.1276

Hyatt, A. D., Boyle, D. G., Olsen, V., Boyle, D. B., Berger, L., Obendorf, D., … Colling, A. (2007). Diagnostic assays and sampling protocols for the detection of *Batrachochytrium dendrobatidis*. Diseases of Aquatic Organisms, 73(3), 175-192. doi: 10.3354/dao073175

Johnson, M. L., Berger, L., Philips, L. & Speare, R. (2003). Fungicidal effects of chemical disinfectants, UV light, desiccation and heat on the amphibian chytrid *Batrachochytrium dendrobatidis*. Disease of Aquatic Organisms, 57(3): 255-260. doi: 10.3354/dao057255

Kärvemo, S., Meurling, S., Berger, D., Höglung, J., & Laurila, A. (2018). Effects of host species and environmental factors on the prevalence of *Batrachochytrium dendrobatidis* in northern Europe. PLoS ONE, 13(10), e0199852. doi: 10.1371/journal.pone.0199852

Kendell, K. (2003). Status of the northern leopard frog (*Rana pipiens*) in Alberta: update 2003. Alberta Sustainable Resource Development, Fish and Wildlife Division, and Alberta Conservation Association, Wildlife Status Report, (9).

557 Klaus, S. P., & Lougheed, S. C. (2013). Changes in breeding phenology of eastern
558 Ontario frogs over four decades. Ecology and Evolution, 3(4), 835-845.
559 doi: 10.1002/ece3.501

560 Kriger, K. M., & Hero, J. M. (2007). The chytrid fungus *Batrachochytrium*
561 *dendrobatidis* is non-randomly distributed across amphibian breeding habitats.
562 Diversity and Distributions, 13(6), 781-788. doi: 10.1111/j.1472-4642.2007.00394.x

563 Kriger, K. M., Pereoglou, F., & Hero, M. (2007). Latitudinal variation in the prevalence
564 and intensity of chytrid (*Batrachochytrium dendrobatidis*) infection in eastern
565 Australia. Conservation Biology, 21(5), 1280-1290. doi: 10.1111/j.1523-
566 1739.2007.00777.x

567 Lambrechts L., Chavatte J. -M., Snounou G., & Koella J. C. (2006). Environmental
568 influence on the genetic basis of mosquito resistance to malaria parasites. Proceedings
569 of the Royal Society of London. Series B: Biological Sciences, 273(1593), 1501-1506.
570 doi: 10.1098/rspb.2006.3483

571 Lampo, M., Rodriguez-Contreras, A., La Marca, E., & Daszak, P. (2006). A
572 chytridiomycosis epidemic and a severe dry season precede the disappearance of
573 Atelopus species from the Venezuelan Andes. Herpetological Journal, 16(14), 395-402.

574 Lehner, B., Verdin, K., & Jarvis, A. (2008). New global hydrography derived from
575 spaceborne elevation data. Eos, Transactions American Geophysical Union, 89(10), 93-
576 94. doi: 10.1029/2008EO100001

577 Lesbarrères, D., Primmer, C. R., Lodé, T., & Merilä, J. (2006). The effects of 20 years
578 of highway presence on the genetic structure of Rana dalmatina populations.
579 Ecoscience, 13(4), 531-538. doi: 10.2980/1195-
580 6860(2006)13[531:TEOYOH]2.0.CO;2

581 Lips, K. R., Brem, F., Brenes, R., Reeve, J. D., Alford, R. A., Voyles, J., … Collins, J.
582 P. (2006). Emerging infectious disease and the loss of biodiversity in a Neotropical
583 amphibian community. Proceedings of the National Academy of Sciences of the USA,
584 103(9), 3165-3170. doi: 10.1073/pnas.0506889103

585 Longcore, J., Pessier, A., & Nichols, D. (1999). *Batrachochytrium dendrobatidis* gen.
586 et sp. nov., a chytrid pathogenic to amphibians. Mycologia, 91(2), 219-227. doi:
587 10.2307/3761366

588 McMillan, K. M., Lesbarrères, D., Harrison, X. A., & Garner, T. W. J. (2019). Data
589 from: Spatiotemporal heterogeneity decouples infection parameters of amphibian
590 chytridiomycosis. Figshare, https://figshare.com/account/home#/projects/71426

591 O'Hanlon, S. J., Rieux, A., Farrer, R. A., Rosa, G. M., Waldman, B., Bataille, A., …
592 Fisher, M. C. (2018). Recent Asian origin of chytrid fungi causing global amphibian
593 declines. Science, 360(6389), 621-627. doi: 10.1126/science.aar1965

594 Olson, D. H., Aanensen, D. M., Ronnenberg, K. L., Powell, C. I., Walker, S. F., Bielby,
595 J., … Weaver, G., The Bd Mapping Group & Fisher, M. C. (2013). Mapping the global
596 emergence of *Batrachochytrium dendrobatidis*, the amphibian chytrid fungus. PLoS
597 ONE, 8(2), e56802. doi: 10.1371/journal.pone.0056802

598 Ostfeld, R. S., Glass, G. E., & Keesing, F. (2005). Spatial epidemiology: an emerging
599 (or re-emerging) discipline. Trends in Ecology and Evolution, 20(6), 328-336. doi:
600 10.1016/j.tree.2005.03.009

601 Paaijmans, K. P., Read, A. F., & Thomas, M. B. (2009). Understanding the link between
602 malaria risk and climate. Proceedings of the National Academy of Sciences of the USA,
603 106(33), 13844-13849. doi: 10.1073/pnas.0903423106

604 Phillott, A. D., Speare, R., Hines, H. B., Skerratt, L. F., Meyer, E., McDonald, K. R.,
605 … Berger, L. (2010). Minimising exposure of amphibians to pathogens during field
606 studies. Diseases of Aquatic Organisms, 92(2-3), 175-185. doi: 10.3354/dao02162

607 Piotrowski, J. S., Annis, S. L., & Longcore, J. E. (2004). Physiology of
608 *Batrachochytrium dendrobatidis*, a chytrid pathogen of amphibians. Mycologia, 96(1),
609 9-15. doi: 10.2307/3761981

610 Pounds, J. A., Bustamante, M. R., Coloma, L. A., Consuegra, J. A., Fogden, M. P. L.,
611 Foster, P. N., … Young, B. E. (2006). Widespread amphibian extinctions from
612 epidemic disease driven by global warming. Nature, 439(7073), 161-167. doi:
613 10.1038/nature04246

614 Puschendorf, R., Carnaval, A. C., VanDerWal, J., Zumbado-Ulate, H., Chaves, G.,
615 Bolaños, F., & Alford, R. A. (2009). Distribution models for the amphibian chytrid
616 *Batrachochytrium dendrobatidis* in Costa Rica: proposing climatic refuges as a
617 conservation tool. Diversity and Distributions, 15(13), 401-408. doi: 10.1111/j.1472-
618 4642.2008.00548.x

619 R Core Team (2015). R: A language and environment for statistical computing: R
620 Foundation for Statistical Computing. Vienna, Austria, 3(0). Available: http://www.r-
621 project.org/ [accessed 2012 January 5].

622 Raffel, T. R., Rohr, J. R., Kiesecker, J. M., & Hudson, P. J. (2006). Negative effects of
623 changing temperature on amphibian immunity under field conditions. Functional
624 Ecology, 20(5), 819-828. doi: 10.1111/j.1365-2435.2006.01159.x

625 Richards, S. A., Whittingham, M. J., & Stephens, P. A. (2011). Model selection and
626 model averaging in behavioural ecology: the utility of the IT-AIC framework.
627 Behavioral Ecology and Sociobiology. 65(1), 77–89. doi: 10.1007/s00265-010-1035-8

628 Rohr, J. R., Dobson, A. P., Johnson, P. T., Kilpatrick, A. M., Paull, S. H., Raffel, T. R.,
629 … Thomas, M. B. (2011). Frontiers in climate change-disease research. Trends in
630 Ecology and Evolution, 26(6), 270-277. doi: 10.1016/j.tree.2011.03.002

631 Ron, S. (2005). Predicting the distribution of the amphibian pathogen
632 *Batrachochytrium dendrobatidis* in the New World. Biotropica, 37(2), 209-221. doi:
633 10.1111/j.1744-7429.2005.00028.x

634 Ruggeri, J., de Carvalho-e-Silva, S. P., James, T. Y., & Toledo, L. F. (2018).
635 Amphibian chytrid infection is influenced by rainfall seasonality and water availability.
636 Diseases of Aquatic Organisms, 127(2), 107-115. doi: 10.3354/dao03191

637 Sapsford, S. J., Alford, R. A., & Schwarzkopf, L. (2013). Elevation, temperature, and
638 aquatic connectivity all influence the infection dynamics of the amphibian chytrid
639 fungus in adult frogs. PLoS ONE, 8, e82425. doi: 10.1371/journal.pone.0082425

640 Scheele, B. C., Pasmans, F., Skerratt, L. F., Berger, L., Martel, A., Beukema, W., …
641 De la Riva, I. (2019). Amphibian fungal panzootic causes catastrophic and ongoing loss
642 of biodiversity. Science, 363(6434), 1459-1463. doi: 10.1126/science.aav0379

643 Seburn, C. N. L. (1992). Management plan for the Northern Leopard Frog in Alberta.
644 Unpublished report, Alberta Forestry, Lands and Wildlife, Edmonton, AB, p. 52.

645 Spitzen-van der Sluijs, A., Canessa, S., Martel, A., & Pasmans, F. (2017). Fragile
646 coexistence of a global chytrid pathogen with amphibian populations is mediated by
647 environment and demography. Proceedings of the Royal Society of London. Series B:
648 Biological Sciences, 284(1864), 20171444. doi: 10.1098/rspb.2017.1444

649 St-Amour, V., Wong, W. M., Garner, T. W. J., & Lesbarrères, D. (2008).
650 Anthropogenic influence on prevalence of 2 amphibian parasites. Emerging Infectious
651 Diseases, 14(7), 1175-1176. doi: 10.3201/eid1407.070602

652 Statistics Canada (2011). Rivers (lines), 2011 Census – Boundary files (water file,
653 ghy_000d11a_e.zip). Arc Info Edition. Available: https://www12.statcan.gc.ca/census-
654 recensement/2011/geo/bound-limit/bound-limit-2011-eng.cfm [accessed: 2015
655 November 20]. System requirements: Arc Info Interchange for Windows.

656 Stebbins, R. C. (2003). A field guide to western reptiles and amphibians (3rd ed.).
657 Houghton Mif in Company, Boston, MA.

658 Tobler, U., Borgula, A., & Schmidt, B. R. (2012). Populations of a susceptible
659 amphibian species can grow despite the presence of a parasitic chytrid fungus. PLoS
660 ONE, 7(4), e34667. doi: 10.1371/journal.pone.0034667

661 Voordouw, M. J., Adama, D., Houston, B., Govindarajulu, P., & Robinson, J. (2010).
662 Prevalence of the pathogenic chytrid fungus, *Batrachochytrium dendrobatidis*, in an
663 endangered population of northern leopard frogs, *Rana pipiens*. BMC Ecology, 10(1),
664 6. doi: 10.1186/1472-6785-10-6

665 Walther, G. R., Post, E., Convey, P., Menzel, A., Parmesan, C., Beebee, T. J. C., …
666 Bairlein, F. (2002). Ecological responses to recent climate change. Nature, 416(6879),
667 389-395. doi: 10.1038/416389a

668 Waye, H. L., & Cooper, J. M. (2000). Status of the Northern leopard frog (*Rana pipiens*)
669 in the Creston Valley Wildlife Management Area 1999. Report to the Columbia Basin
670 Fish and Wildlife Compensation Program. Nelson, BC.

671 Wilber, M. Q., Knapp, R. A., Toothman, M., & Briggs, C. J. (2017). Resistance,
672 tolerance and environmental transmission dynamics determine host extinction risk in a
673 load-dependent amphibian disease. Ecology Letters, 20(9), 1169-1181. doi:
674 10.1111/ele.12814

675 Woodhams, D. C., Alford, R. A., Briggs, C. J., Johnson, M., & Rollins-Smith, L. A.

(2008). Life-history trade-offs influence disease in changing climates: strategies of an amphibian pathogen. Ecology, 89(6), 1627-1639. doi: 10.1890/06-1842.

Wright, A. H., & Wright, A. A. (1949). Handbook of frogs and toads of the United States and Canada (3rd ed.). Comstock Publishing Associates, Ithaca, New York.

Xie, G. Y., Olson, D. H., & Blaustein, A. R. (2016). Projecting the global distribution of the emerging amphibian fungal pathogen, *Batrachochytrium dendrobatidis*, based on IPCC climate futures. PLoS ONE, 11(8), e0160746. doi: 10.1371/journal.pone.016074

Yuan, Z., Zhou, W., Chen, X., Poyarkov, N. A., Chen, H., Jang-Liaw, N., … Che, J. (2016). Spatiotemporal diversification of the true frogs (genus Rana): a historical framework for a widely studied group of model organisms. Systematic Biology, 65(5), 824-842. doi: 10.1093/sysbio/syw05

Fig. 1. *Bd* infection prevalence (%) in *R. pipiens* populations collected from 41 sites in Ontario from 2012-2014 (includes the 14 repeat sites). Pie chart denotes prevalence (red: *Bd* +ve, blue: *Bd* -ve), with sample size noted in brackets. Data loggers symbolized by orange markers, weather stations symbolized by green.

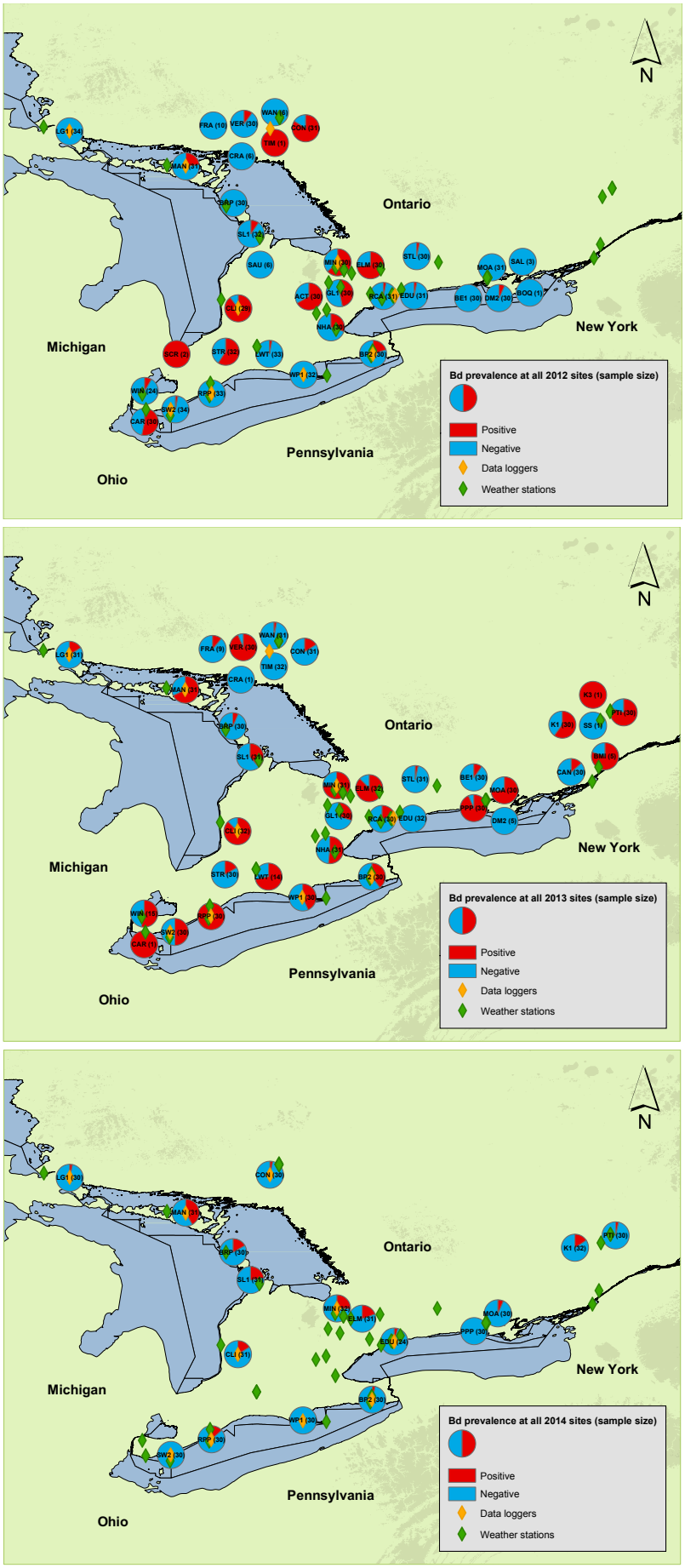

Fig. 2. Stacked bar charts representing the *Bd* prevalence (%) and infection intensity (GE), by year, for the 14 repeat sites (with at least 24 frogs sampled per year). Within a site, % of individuals are grouped by *Bd* intensity categories (including *Bd* negative).

Table 1. Summary statistics for mean daily air temperature (˚C) and mean precipitation (mm) throughout both: active period and breeding period, within all sample years.

	Mean daily air temperature (˚C) throughout active period				Mean daily air temperature (˚C) throughout breeding period				Mean precipitation (mm) throughout active period				Mean precipitation (mm) throughout breeding period			
	$\bar{x}$	se	max	range	$\bar{x}$	se	max	range	$\bar{x}$	se	max	range	$\bar{x}$	se	max	range
2012	7.7	0.2	10.2	4.4	17.1	0.3	19.4	7.2	66.3	1.0	76.5	20.5	72.6	0.9	81.0	18.5
2013	6.9	0.2	11.7	6.8	16.0	0.2	20.4	7.8	69.5	1.3	88.0	31.0	73.0	1.1	86.5	23.0
2014	7.5	0.2	9.8	4.1	17.5	0.2	20.3	5.7	66.3	1.2	76.5	17.5	72.0	1.3	80.0	17.5

Table 2. Summary statistics for spring onset (decimal date), calling date (decimal date) and active period (days), from 2011 to 2015.

	Spring onset (decimal date)					Calling date (decimal date)					Active period (days)				
	$\bar{x}$	se	max	mode	range	$\bar{x}$	se	max	mode	range	$\bar{x}$	se	max	mode	range
2011	90.36	1.75	111	88	44	145.58	1.82	164	148	39	55.21	2.03	80	60	43
2012	71.18	0.69	92	71	26	119.79	4.91	165	138	94	48.61	4.80	94	67	92
2013	99.03	1.83	122	94	41	123.76	2.02	157	120	40	24.73	2.19	64	26	59
2014	95.60	1.76	108	107	22	136.12	1.26	149	138	28	40.52	1.73	62	52	43
2015	91.18	1.29	98	97	31	125.06	2.58	164	118	64	33.88	3.16	74	30	69

Table 3. Spring onset (decimal date), calling date (decimal date) and active period (days), by year. $\mathbf{Y_D}$, difference in decimal dates between current year and the previous year; $\mathbf{\%_V}$, percentage change between current year and the previous year; $\mathbf{T_V}$, total inter-annual variation in decimal days irrespective of directionality; $\mathbf{T_{VD}}$, total inter-annual variation in decimal days respective of directionality; $\mathbf{T_{VD}/\ Y}$, average variation per annum in decimal days, respective of directionality

	Spring onset (decimal date), by year			Calling date (decimal date), by year			Active period (days), by year		
	$\bar{x}$ decimal date	Y_D	$\%_V$	Decimal date	Y_D	$\%_V$	Days	Y_D	$\%_V$
2011	90.36			145.58			55.21		
2012	71.18	-19.18	-21.22	119.79	-25.79	-17.72	48.61	-6.60	-11.95
2013	99.03	+27.85	+39.13	123.76	+3.97	+3.31	24.73	-23.88	-49.12
2014	95.61	-3.42	+3.45	136.12	+12.36	+9.99	40.52	+15.79	+63.85
2015	91.18	-4.43	+4.63	125.06	-11.06	-8.13	33.88	-6.64	-16.39
$\mathbf{T_V}$		54.88			53.18			52.91	
$\mathbf{T_{VD}}$		+0.82			-20.52			-21.33	
$\mathbf{T_{VD}/\ Y}$		+0.21			-5.13			-5.33	

Table 4. Model averaged estimates and confidence intervals (2.5% and 97.5%) for the models in the delta-6 top model set remaining after the nesting rule has been applied, for both *Bd* prevalence (%; models remaining = 4) and *Bd* intensity of infection (GE; models remaining = 3). Calculated using both: (1) conditional average: averages over the models where the parameter appears, and (2) full average: model averaged estimates calculated using the 'zeroes' method where estimates are set to zero in models where they do not occur. 'Importance': relative variable importance, calculated as the sum of the Akaike weights of the models in which that term occurred.

	Importance	Conditional			Full		
		Estimate	2.5%	97.5%	Estimate	2.5%	97.5%
***Bd* prevalence**							
intercept	-	-1.502	-2.422	-0.582	-1.502	-2.422	-0.582
factor(year)2013	1.00	1.248	0.572	1.925	1.248	0.572	1.925
factor(year)2014	1.00	-1.109	-1.654	-0.564	-1.109	-1.654	-0.564
active period length	0.39	-0.274	-0.092	0.639	-0.085	-0.236	0.406
active period mean temperature	0.73	-0.349	-0.532	0.167	-0.214	-0.577	0.148
active period length * active period mean temperature	0.39	0.245	0.018	0.509	0.076	-0.190	0.343
breeding period mean temperature	0.39	0.362	0.167	0.556	0.075	-0.226	0.377
***Bd* intensity of infection**							
intercept	-	2.275	0.858	3.693	2.275	0.858	3.693
factor(year)2013	1.00	1.840	0.365	3.316	1.840	0.365	3.316
factor(year)2014	1.00	-1.731	-3.167	-0.294	-1.731	-3.167	-0.294
river density	0.56	0.232	-0.701	1.165	0.109	-0.571	0.791
breeding period mean precipitation	0.56	0.322	-0.511	1.155	0.152	-0.502	0.807
hydroshed area	0.96	-2.195	-6.008	1.618	-2.080	-5.913	0.753
river density * breeding period mean precipitation	0.56	1.533	0.210	2.857	0.727	-1.029	2.482

Fig. 3. Model predicted relationship between *Bd* prevalence (%) and the following interaction: mean daily air temperature (˚C) during active period (negatively correlated) and length of active period (days; positively correlated). The three lines represent the relationship between *Bd* prevalence and mean daily air temperature during the active period when length of active period is held at: i) its global mean (sold black line), ii) one standard deviation below the global mean (dotted line, light green shaded area spans the 95% credible intervals for the fitted means), iii) one standard deviation above the global mean (long dashed line, dark green shaded area spans the 95% credible intervals for the fitted means). Variation in *Bd* prevalence is greatest when active periods are shortened and temperatures are cool. If active periods are extended, the relationship between *Bd* prevalence and mean daily air temperature diminishes. However, if active periods are shortened, this relationship becomes more negative.

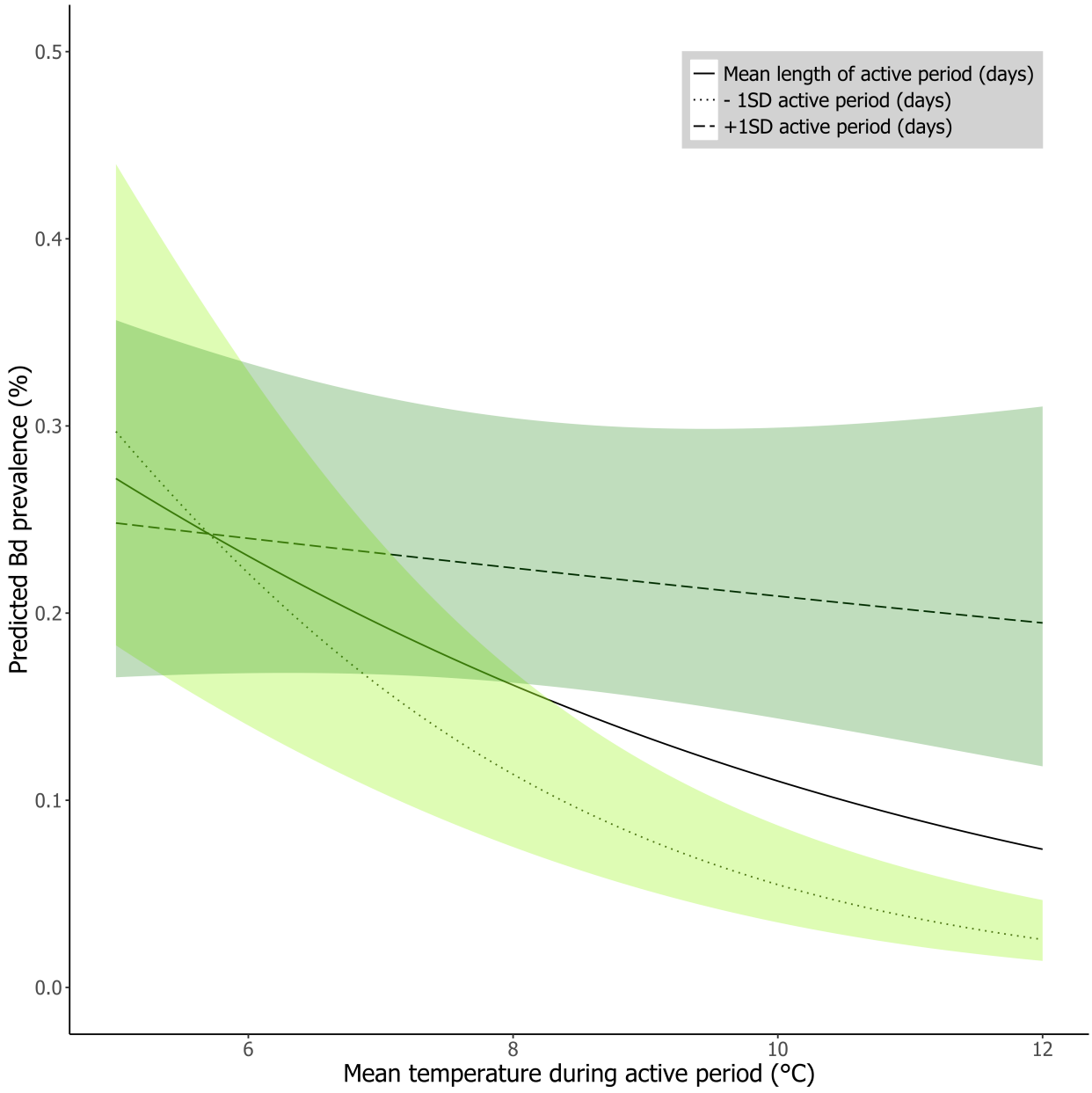

Fig. 4. Model predicted relationship between *Bd* mean intensity (GE) and hydroshed area (km²). After an initial rapid exponential decrease, mean infection intensity reaches a plateau at very low intensities/ zero infection at approximately 20,000 km².

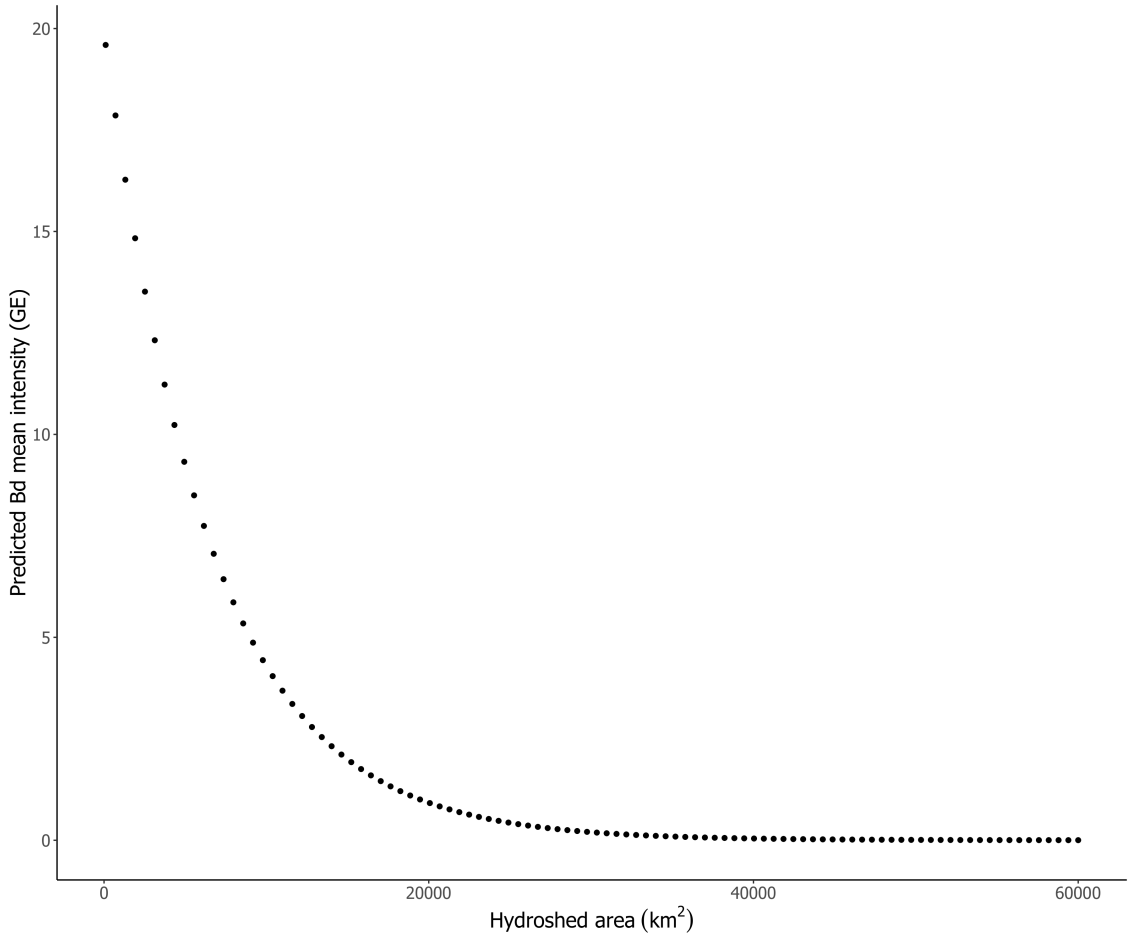

Fig. 5. Model predicted relationship between *Bd* mean intensity (GE) and the following interaction: river density (within 10 km buffer from site centroid; positively correlated) and mean precipitation (mm) throughout breeding period (positively correlated). The three lines represent the relationship between *Bd* mean intensity and mean precipitation throughout breeding period, when river density is held at: i) its global mean (sold black line, orange shaded area spans the 95% credible intervals for the fitted means), ii) one standard deviation below the global mean (dotted line), iii) one standard deviation above the global mean (long dashed line). *Bd* mean intensity is greatest when a site locality is in close proximity to a dense network of rivers, and precipitation is high. If river densities are low, *Bd* mean intensity increases slightly when precipitation levels are low.

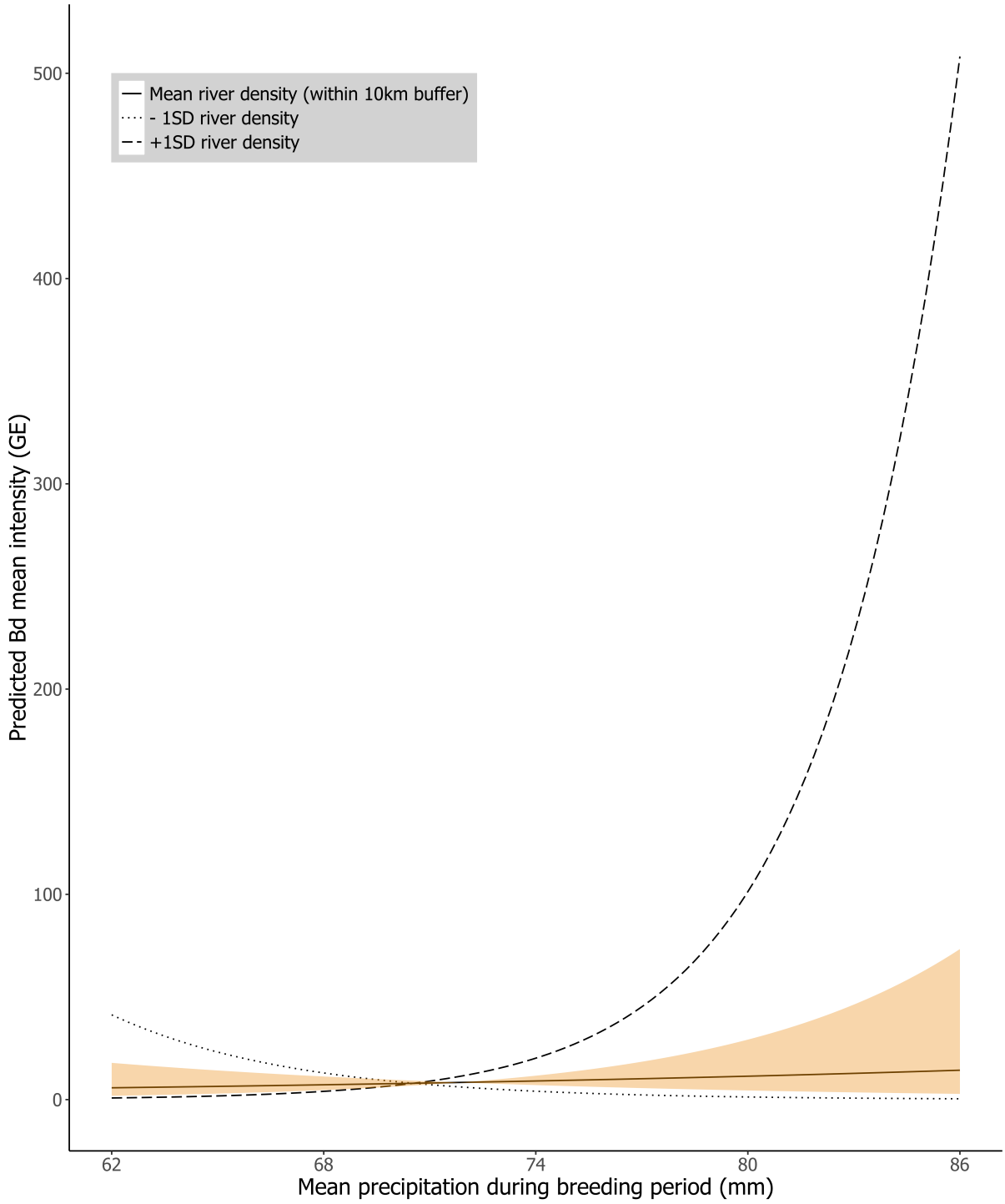

Fig. S1. The distribution of the *R. pipiens* throughout Ontario. Includes both historic and recent observations compiled from data recorded by Bird Studies Canada: Marsh Monitoring Program, and Ontario Nature: Ontario Reptile and Amphibian Atlas and the Original Herpetofaunal Summary. Atlas squares are based on a 5 x 5 km grid. Areas without squares do not indicate the absence of the species, but only that there are no observation data to confirm the presence of the species in those areas.

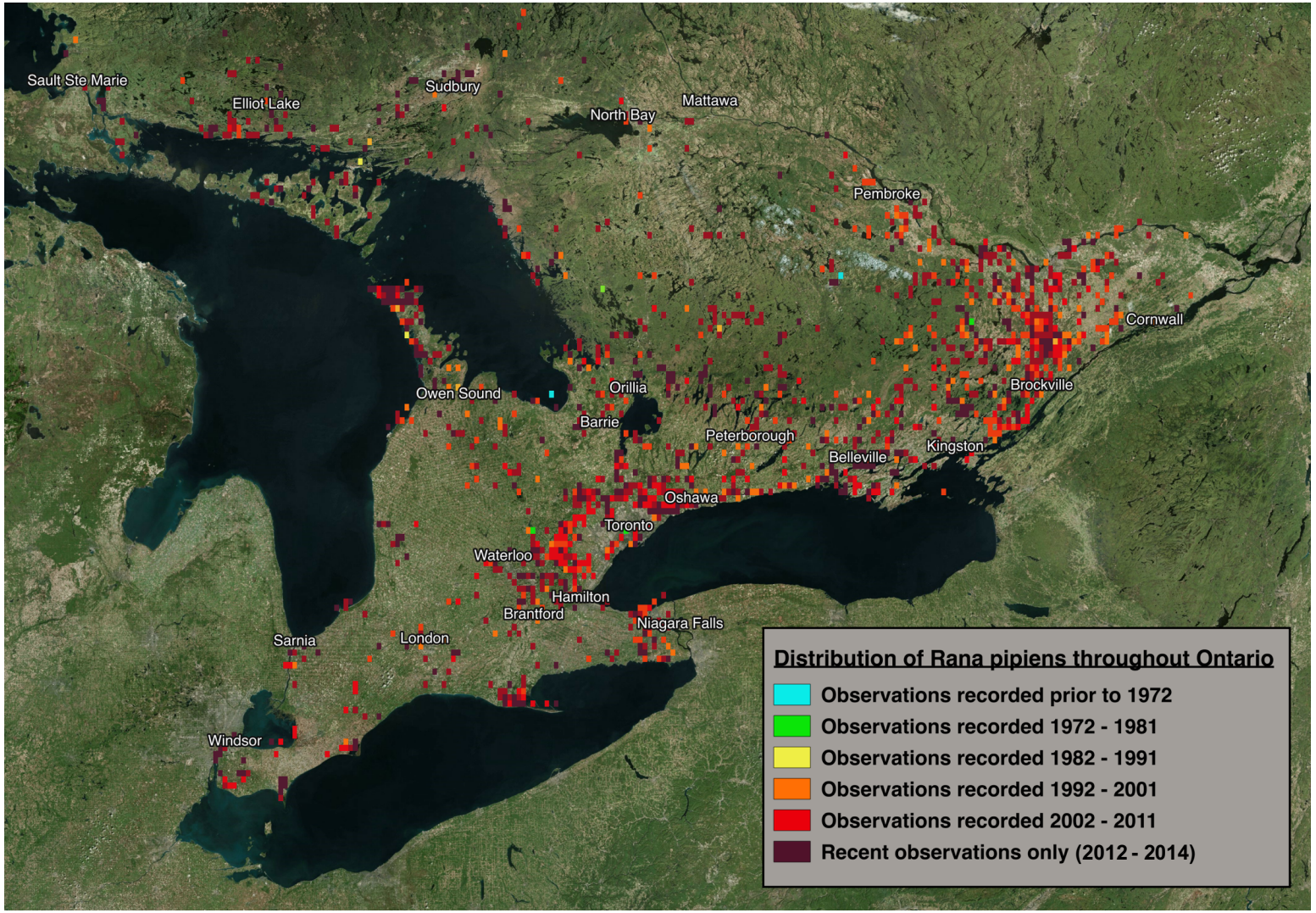

Fig. S2. Stacked bar charts representing *Bd* prevalence (%) and infection intensity (GE), by year. Individual counts of infection intensity are labeled in blue; proportion of infected and non-infected individuals are labeled as percentages; and samples sizes are denoted on top. Note greater prevalence and higher infection intensity recorded in 2013.

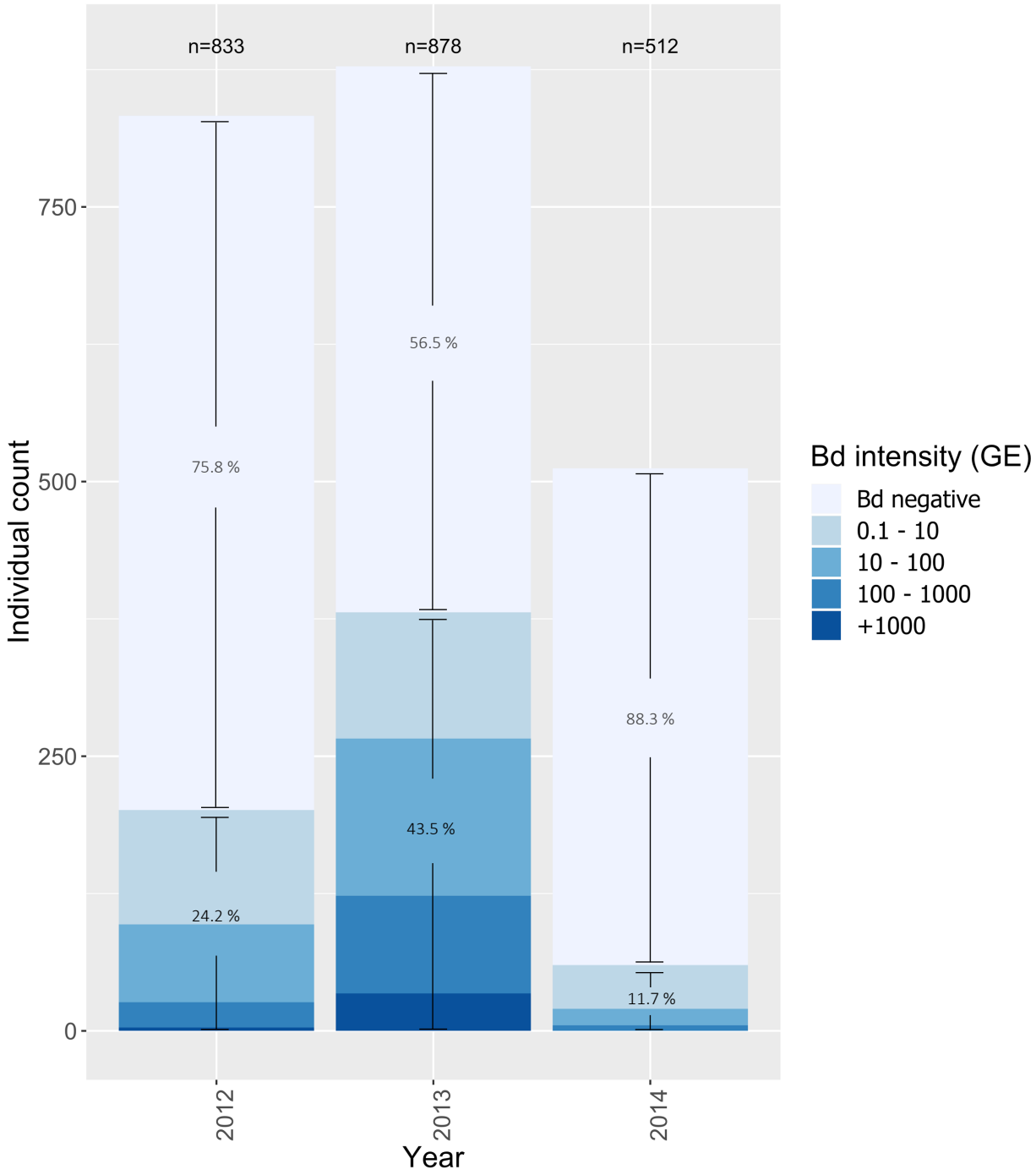

Fig. S3. Density plot of log *Bd* intensity (GE), by year. Note the lower density of zero/ low infections in 2013, in comparison to 2012 and 2014, and again a greater density of strong infections in 2013, in comparison to 2012 and 2014.

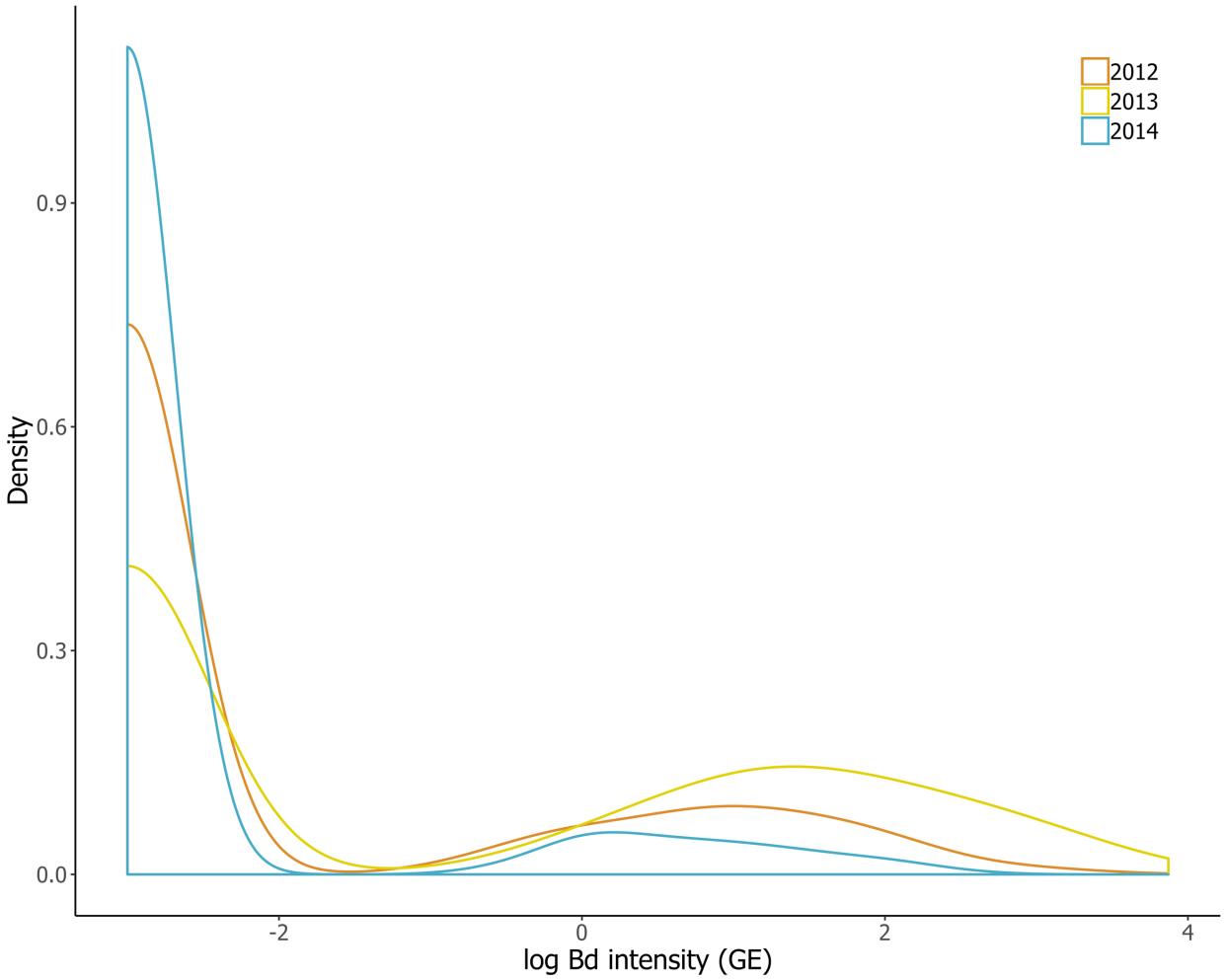

Table S1. *Bd* prevalence (%) and infection intensity (GE) in *R. pipiens* populations collected from 41 sites in Ontario from 2012-2014. The 14 sites repeat sampled during late summer (with at least 24 frogs sampled per year) are highlighted in the far-right column.

Site	Year	Sample size	% Prevalence (N = Individuals *Bd* positive)	Mean infection intensity (SE, range)	Temperature and precipitation data compiled (logger or weather station)	Repeat sampled
ACT	2012	30	66.7 (20)	104.92 (89.9, 0.21 - 2708.28)	✓	
BE1	2012	30	0 (0)	0	✓	
	2013	30	10 (3)	0.24 (0.17, 0.56 - 4.83)	✓	
BMI	2013	5	80 (4)	22.34 (18.82, 0.56 - 97.31)	✗	
BOQ	2012	1	0 (0)	0	✗	
BP2	2012	30	20 (6)	1.0 (0.49, 0.52 - 11.63)	✓	
	2013	30	40 (12)	20.25 (7.99, 1.98 - 199.09)	✓	*
	2014	30	3.3 (1)	4.01 (4.01, 120.44 - 120.44)	✓	*
BRP	2012	30	0 (0)	0	✓	*
	2013	30	6.7 (2)	0.08 (0.07, 0.32 - 2.09)	✓	*
	2014	30	16.7 (5)	2.42 (1.39, 2.93 - 35.79)	✓	*
CAN	2013	30	13.3 (4)	0.74 (0.49, 0.47 - 11.41)	✓	
CAR	2012	30	53.3 (16)	3.9 (1.79, 0.14 - 42.39)	✓	
	2013	1	100 (1)	0.32 (0, 0.32 - 0.32)	✓	
CLI	2012	29	89.7 (26)	51.47 (22.75, 0.52 - 622.49)	✓	*
	2013	32	87.5 (28)	158.27 (54.84, 0.65 - 1323.62)	✓	*
	2014	31	16.1 (5)	0.78 (0.4, 0.98 - 7.72)	✓	*
CON	2012	31	83.9 (26)	127.8 (46.65, 0.92 - 1022.6)	✓	*
	2013	31	16.1 (5)	0.25 (0.18, 0.3 - 5.49)	✓	*
	2014	30	3.3 (1)	0.09 (0.09, 2.6 - 2.6)	✓	*
CRA	2012	6	0 (0)	0	✗	
	2013	1	0 (0)	0	✗	
DM2	2012	30	6.7 (2)	1.45 (1.45, 0.09 - 43.47)	✓	
	2013	5	0 (0)	0	✓	
EDU	2012	31	3.2 (1)	0.05 (0.05, 1.52 - 1.52)	✓	*
	2013	32	0 (0)	0	✓	*
	2014	24	4.2 (1)	1.27 (1.27, 30.47 - 30.47)	✓	*
ELM	2012	30	73.3 (22)	8.46 (2.63, 0.12 - 58.69)	✓	*
	2013	32	87.5 (28)	484.97 (141.23, 3.61 - 3371.34)	✓	*
	2014	31	19.4 (6)	5.95 (4.23, 0.24 - 116.57)	✓	*

Site	Year	Sample size	% Prevalence (N = Individuals *Bd* positive)	Mean infection intensity (SE, range)	Temperature and precipitation data compiled (logger or weather station)	Repeat sampled
FRA	2012	10	0 (0)	0	✗	
	2013	9	11.1 (1)	0.08 (0.08, 0.72 - 0.72)	✗	
GL1	2012	30	46.7 (14)	21.7 (9.86, 0.27 - 256.42)	✓	
	2013	30	30 (9)	5.7 (3.43, 0.83 - 96.61)	✓	
K1	2013	30	60 (18)	42.24 (15.66, 0.29 - 426.67)	✓	
	2014	32	15.6 (5)	0.92 (0.51, 1.29 - 14.77)	✓	
K3	2013	1	100 (1)	20.76 (0, 20.76 - 20.76)	✗	
LG1	2012	34	0 (0)	0	✓	*
	2013	31	16.1 (5)	0.43 (0.31, 0.02 - 9.25)	✓	*
	2014	30	3.3 (1)	0.04 (0.04, 1.13 - 1.13)	✓	*
LWT	2012	33	3 (1)	0.45 (0.45, 14.97 - 14.97)	✓	
	2013	14	71.4 (10)	25.12 (15.72, 1.15 - 221.86)	✓	
MAN	2012	31	22.6 (7)	16.39 (8.33, 2.58 - 167.84)	✓	*
	2013	31	67.7 (21)	36.01 (12.98, 0.84 - 307.94)	✓	*
	2014	31	41.9 (13)	7.05 (3.93, 0.57 - 117.91)	✓	*
MIN	2012	30	63.3 (19)	9.34 (3.8, 0.18 - 100.78)	✓	*
	2013	31	74.2 (23)	39.87 (14.28, 1.48 - 424.68)	✓	*
	2014	32	25 (8)	0.72 (0.35, 0.35 - 7.93)	✓	*
MOA	2012	31	0 (0)	0	✓	*
	2013	30	73.3 (22)	149.52 (85.62, 0.58 - 2407.03)	✓	*
	2014	30	6.7 (2)	10.43 (10.41, 0.67 - 312.27)	✓	*
NHA	2012	30	30 (9)	2.31 (1.16, 0.27 - 26.43)	✓	
	2013	31	51.6 (16)	121.64 (51.47, 4.69 - 1400.91)	✓	
PPP	2013	30	93.3 (28)	1001.34 (292.82, 1.08 - 7427.23)	✓	
	2014	30	0 (0)	0	✓	
PTI	2013	30	80 (24)	486.15 (176.71, 0.43 - 4166.62)	✓	
	2014	30	3.3 (1)	2.6 (2.6, 78.09 - 78.09)	✓	
RCA	2012	31	3.2 (1)	4.4 (4.4, 136.48 - 136.48)	✓	
	2013	30	20 (6)	63.39 (58.13, 2.61 - 1746.99)	✓	
RPP	2012	33	0 (0)	0	✓	*
	2013	30	93.3 (28)	216.69 (60.06, 3.79 - 1230.34)	✓	*
	2014	30	13.3 (4)	0.93 (0.59, 0.82 - 15.19)	✓	*
SAL	2012	3	0 (0)	0	✗	
SAU	2012	6	0 (0)	0	✗	

Site	Year	Sample size	% Prevalence (N = Individuals *Bd* positive)	Mean infection intensity (SE, range)	Temperature and precipitation data compiled (logger or weather station)	Repeat sampled
SCR	2012	2	100 (2)	343.73 (342.78, 0.95 - 686.51)	✗	
SL1	2012	32	9.4 (3)	6.6 (4.12, 41.12 - 117.01)	✓	*
	2013	31	38.7 (12)	6.16 (3.1, 0.16 - 91.78)	✓	*
	2014	31	22.6 (7)	9.09 (4.92, 0.41 - 138.03)	✓	*
SS	2013	1	0 (0)	0	✗	
STL	2012	30	3.3 (1)	0.02 (0.02, 0.59 - 0.59)	✓	
	2013	31	3.2 (1)	0.1 (0.1, 3.22 - 3.22)	✓	
STR	2012	32	59.4 (19)	65.95 (46.1, 0.6 - 1479.94)	✓	
	2013	30	16.7 (5)	3.88 (3.36, 1.33 - 101.02)	✓	
SW2	2012	34	2.9 (1)	9.79 (9.79, 332.92 - 332.92)	✓	*
	2013	30	50 (15)	45.84 (20.67, 3.37 - 528.43)	✓	
	2014	30	0 (0)	0	✓	*
TIM	2012	1	100 (1)	0.85 (0, 0.85 - 0.85)	✓	
	2013	32	0 (0)	0	✓	
VER	2012	30	10 (3)	0.41 (0.33, 0.87 - 9.89)	✓	
	2013	30	93.3 (28)	1062.49 (290.73, 4.14 - 6221.99)	✓	
WAN	2012	6	0 (0)	0	✓	
	2013	31	3.2 (1)	1.64 (1.64, 50.99 - 50.99)	✓	
WIN	2012	24	8.3 (2)	0.46 (0.43, 0.69 - 10.41)	✓	
	2013	15	53.3 (8)	5.87 (2.3, 0.77 - 29.9)	✓	
WP1	2012	32	0 (0)	0	✓	*
	2013	30	43.3 (13)	45.49 (22.89, 2.7 - 601.2)	✓	*
	2014	30	0 (0)	0	✓	*
TOTAL		2223 (41 sites, 87 visits)	28.9 (644)	61.79 (7.82, 0.02 - 7427.23)	32 sites (76 visits)	14 sites (40 visits)

Table S2. Spatial predictor variables selected for use in model building based on their suitability for hypothesis testing. Details regarding the variations (per grid cell), raw resolutions, year of record, unit, source, prediction and predicted relationship for all spatial predictors. "+" and "–" represent an expected positive or negative correlation, respectively.

Predictor	Variations (per grid cell)	Raw resolution	Year recorded	Unit	Source	Prediction	Predicted relationship	Support for prediction
Hydroshed area	total	30 arc seconds (~1 km)	2008	km^2	'USGS HyrdoSHEDS' http://hydrosheds.cr.usgs.gov Lehner et al., 2008	As water basins serve as likely vectors for the waterborne *Bd* zoospores, an increase in basin size will lower infection parameters due to diluted pathogen concentrations.	-	[1-4]
River density	mean	1 x 1 km (10 km mean extracted)	2011	km	'2011 Census -Rivers (lines)' https://www12.statcan.gc.ca/census-recensement/2011/geo/bound-limit/bound-limit-2011-eng.cfm Statistics Canada, 2011	Infection parameters will be greatest in areas with dense river networks, as it provides increased transmission channels via aquatic nodes.	+	[5-7]
Precipitation (during breeding period)	mean	30 arc seconds (~1 km)	1950 - 2000	mm	'Current Conditions: Precipitation' http://www.worldclim.org Hijmans et al., 2005	Infection parameters will increase with increased precipitation, as water must be present for *Bd* to infect new hosts or to re-infect current hosts.	+	[7-9]
Precipitation (during active period)								
Air temperature (during active period)	mean	N/A	2011 - 2015	°C	Calculated from data loggers and historical data from weather stations (see Fig. S1). http://climate.weather.gc.ca/historical_data/search_historic_data_e.html Government of Canada, 2015a	Infection parameters will increase as temperatures decrease.	-	[10-12]
Length of active period (days between spring onset and calling date)	total			days		As length of active period is elongated, infection parameters will increase due to expanded opportunities for successful pathogen transmission.	+	[13]
Road density	mean	1 x 1 km (50 km mean extracted)	2015	mm	'National Road Network (NRN) – Ontario.' https://open.canada.ca/data/en/dataset/3d282116-e556-400c-9306-ca1a3cada77f Government of Canada, 2015b	Increased road density will intensify landscape fragmentation leading to isolated habitat patches and dense host populations, which will allow for an increase in infection parameters.	+	[14-20]

References, relating to Table S2.

1. De Castro, F., & Bolker, B. (2005). Mechanisms of disease-induced extinction. Ecology Letters, 8(1), 117-126. doi: 10.1111/j.1461-0248.2004.00693.x

2. Briggs, C. J., Vredenburg, V. T., Knapp, R. A., & Rachowicz, L. J. (2005). Investigating the population level effects of chytridiomycosis: an emerging infectious disease of amphibians. Ecology, 86(12), 3149-3159. doi: 10.1890/04-1428

3. Rachowicz, L. J., & Briggs, C. J. (2007). Quantifying the disease transmission function: effects of density on Batrachochytrium dendrobatidis transmission in the mountain yellow legged frog Rana muscosa. Journal of Animal Ecology, 76(4), 711-721. doi: 10.1111/j.1365-2656.2007.01256.x

4. Briggs, C. J., Knapp, R. A., & Vredenburg, V. T. (2010). Enzootic and epizootic dynamics of the chytrid fungus pathogen of amphibians. Proceedings of the National Academy of Sciences of the USA, 107(21), 9695-9700. doi: 10.1073/pnas.0912886107

5. Kriger, K. M., & Hero, J. M. (2007). The chytrid fungus Batrachochytrium dendrobatidis is non-randomly distributed across amphibian breeding habitats. Diversity and Distributions, 13(6), 781-788. doi: 10.1111/j.1472-4642.2007.00394.x

6. Sapsford, S. J., Alford, R. A., & Schwarzkopf, L. (2013). Elevation, temperature, and aquatic connectivity all influence the infection dynamics of the amphibian chytrid fungus in adult frogs. PLoS ONE, 8, e82425. doi: 10.1371/journal.pone.0082425

7. Piotrowski, J. S., Annis, S. L., & Longcore, J. E. (2004). Physiology of Batrachochytrium dendrobatidis, a chytrid pathogen of amphibians. Mycologia, 96(1), 9-15. doi: 10.2307/3761981

8. Puschendorf, R., Carnaval, A. C., VanDerWal, J., Zumbado-Ulate, H., Chaves, G., Bolaños, F., & Alford, R. A. (2009). Distribution models for the amphibian chytrid Batrachochytrium dendrobatidis in Costa Rica: proposing climatic refuges as a conservation tool. Diversity and Distributions, 15(13), 401-408. doi: 10.1111/j.1472-4642.2008.00548.x

9. Lips, K. R. (1998). Decline of a tropical montane amphibian fauna. Conservation Biology, 12(1), 106-117. doi: 10.1111/j.1523-1739.1998.96359.x

10. Berger, L., Speare, R., Hines, H. B., Marantelli, G., Hyatt, A. D., McDonald, K. R., … Tyler, M. J. (2004). Effect of season and temperature on mortality in amphibians due to chytridiomycosis. Australian Veterinary Journal, 82(7), 434-439. doi: 10.1111/j.1751-0813.2004.tb11137.x

11. Lips, K. R., Brem, F., Brenes, R., Reeve, J. D., Alford, R. A., Voyles, J., … Collins, J. P. (2006). Emerging infectious disease and the loss of biodiversity in a Neotropical amphibian community. Proceedings of the National Academy of Sciences of the USA, 103(9), 3165-3170. doi: 10.1073/pnas.0506889103

12. Woodhams, D. C., & Alford, R. A. (2005). Ecology of chytridiomycosis in rainforest stream frog assemblages of tropical Queensland. Conservation Biology, 19(5), 1449-1459. doi: 10.1111/j.1523-1739.2005.004403.x

13. Lampo, M., Rodriguez-Contreras, A., La Marca, E., & Daszak, P. (2006). A chytridiomycosis epidemic and a severe dry season precede the disappearance of Atelopus species from the Venezuelan Andes. Herpetological Journal, 16(14), 395-402.

14. Balkenhol, N., & Waits, L. P. (2009). Molecular road ecology: exploring the potential of genetics for investigating transportation impacts on wildlife. Molecular Ecology, 18(20), 4151-4164. doi: 10.1111/j.1365-294X.2009.04322.x

15. Gibbs, J. P., & Breisch, A. R. (2001). Climate warming and calling phenology of frogs near Ithaca, New York, 1900 - 1999. Conservation Biology, 15(4), 1175-1178. doi: 10.1046/j.1523-1739.2001.0150041175.x

16. Lesbarrères, D., Pagano, A., & Lodé, T. (2003). Inbreeding and road effect zone in a Ranidae: the case of Agile frog, Rana dalmatina Bonaparte, 1840. Comptes Rendus Biologies, 326, 68-72. doi: 10.1016/S1631-0691(03)00040-4

17. Lesbarrères, D., Primmer, C. R., Lodé, T., & Merilä, J. (2006). The effects of 20 years of highway presence on the genetic structure of Rana dalmatina populations. Ecoscience, 13(4), 531-538. doi: 10.2980/1195-6860(2006)13[531:TEOYOH]2.0.CO;2

18. Vos, C. C., & Chardon, J. P. (1998). Effects of habitat fragmentation and road density on the distribution pattern of the moor frog Rana arvalis. Journal of Applied Ecology, 35(1), 44-56. doi: 10.1046/j.1365-2664.1998.00284.x

19. Houlahan, J. E., & Findlay, C. S. (2003). The effects of adjacent land use on wetland amphibian species richness and community composition. Canadian Journal of Fisheries and Aquatic Sciences, 60, 1078-1094. doi: 10.1139/f03-095

20. St-Amour, V., Wong, W. M., Garner, T. W. J., & Lesbarrères, D. (2008). Anthropogenic influence on prevalence of 2 amphibian parasites. Emerging Infectious Diseases, 14(7), 1175-1176. doi: 10.3201/eid1407.070602

Table S3. Akaike's information criterion model rankings for the candidate models explaining *Bd* prevalence (%) at site level. Quasi-Akaike information criterion (QAIC) was used in order to correct for overdispersion. ***k***, number of parameters; **logLik**, log likelihood; **QAIC**, Akaike's information criterion corrected for small sample size; **ΔQAIC**, difference in QAIC compared with the model with the lowest QAIC; w_i, model weight; **Retained**, models within Δ6 QAIC are not retained if they are more complex versions of nested models with better QAIC support; **year**, year of sample date; **site**, accounted for possible non-independence of samples collected at the same site locality by including this random intercept effect; **active period length**, number of days between onset of spring and calling date; **active period mean temperature**, mean daily air temperature (˚C) throughout active period; **breeding period mean temperature**, mean daily air temperature (˚C) throughout breeding period; **active period mean precipitation**, mean precipitation (mm) throughout active period; **breeding period mean precipitation**, mean precipitation (mm) throughout breeding period; **hydroshed area** (km^2); **river density**, within 10 km buffer from site centroid; **road density**, within 50 km buffer from site centroid.

Model	Model description	*k*	logLik	QAIC	ΔQAIC	*wi*	Retained
m1	factor(year) + active period length * active period mean temperature + (1 | site)	7	-167.08	67.78	0.000	0.107	✓
m20	factor(year) + active period mean temperature + (1 | site)	5	-180.13	67.82	0.042	0.105	✓
m2	factor(year) + active period mean temperature + active period mean precipitation + (1 | site)	6	-174.17	67.97	0.195	0.097	✗
m31	factor(year) + breeding period mean temperature + (1 | site)	5	-182.56	68.57	0.796	0.072	✓
m25	factor(year) + (1 | site)	4	-190.04	68.89	1.113	0.062	✓
m5	factor(year) + active period length * active period mean precipitation + (1 | site)	7	-171.66	69.20	1.420	0.053	✗
m21	factor(year) + active period mean precipitation + (1 | site)	5	-186.02	69.64	1.867	0.042	✗
m3	factor(year) + active period mean temperature + hydroshed area + (1 | site)	6	-179.75	69.70	1.925	0.041	✗
m4	factor(year) + active period mean temperature + river density + (1 | site)	6	-179.78	69.71	1.934	0.041	✗
m18	factor(year) + active period mean temperature + road density + (1 | site)	6	-180.06	69.80	2.023	0.039	✗
m19	factor(year) + breeding period mean precipitation + (1 | site)	5	-187.22	70.02	2.241	0.035	✗
m28	factor(year) + breeding period mean temperature + hydroshed area + (1 | site)	6	-181.89	70.36	2.588	0.029	✗
m29	factor(year) + breeding period mean temperature + river density + (1 | site)	6	-182.21	70.46	2.687	0.028	✗
m27	factor(year) + breeding period mean temperature + breeding period mean precipitation + (1 | site)	6	-182.43	70.53	2.757	0.027	✗
m30	factor(year) + breeding period mean temperature + road density + (1 | site)	6	-182.53	70.56	2.788	0.027	✗
m24	factor(year) + hydroshed area + (1 | site)	5	-189.31	70.66	2.888	0.025	✗
m22	factor(year) + river density + (1 | site)	5	-189.72	70.79	3.016	0.024	✗
m23	factor(year) + road density + (1 | site)	5	-189.96	70.87	3.091	0.023	✗
m6	factor(year) + active period mean precipitation + hydroshed area + (1 | site)	6	-185.40	71.45	3.676	0.017	✗
m17	factor(year) + active period mean precipitation + road density + (1 | site)	6	-185.77	71.57	3.790	0.016	✗
m7	factor(year) + active period mean precipitation + river density + (1 | site)	6	-185.88	71.60	3.826	0.016	✗
m12	factor(year) + breeding period mean precipitation + hydroshed area + (1 | site)	6	-186.10	71.67	3.892	0.015	✗
m16	factor(year) + road density + breeding period mean precipitation + (1 | site)	6	-187.07	71.97	4.193	0.013	✗
m11	factor(year) + river density + breeding period mean precipitation + (1 | site)	6	-187.15	71.99	4.218	0.013	✗
m15	factor(year) + road density * breeding period mean precipitation + (1 | site)	7	-184.07	73.04	5.263	0.008	✗
m9	factor(year) + river density + breeding period mean precipitation + hydroshed area + (1 | site)	7	-185.99	73.63	5.858	0.006	✗
m14	factor(year) + road density + breeding period mean precipitation + hydroshed area + (1 | site)	7	-186.00	73.64	5.863	0.006	✗
m10	factor(year) + river density * breeding period mean precipitation + (1 | site)	7	-186.19	73.70	5.922	0.006	✗
m13	factor(year) + road density * breeding period mean precipitation + hydroshed area + (1 | site)	8	-182.81	74.65	6.874	0.003	✗
m8	factor(year) + river density * breeding period mean precipitation + hydroshed area + (1 | site)	8	-184.68	75.23	7.453	0.003	✗
m26	1 + (1 | site)	2	-269.89	89.64	21.860	0.000	

Table S4. Akaike's information criterion model rankings for the candidate models explaining *Bd* intensity of infection (mean GE) at site level. ***k***, number of parameters; **logLik**, log likelihood; **AIC**, Akaike's information criterion corrected for small sample size; **ΔAIC**, difference in AIC compared with the model with the lowest AIC; w_i, model weight; **Retained**, models within Δ6 AIC are not retained if they are more complex versions of nested models with better AIC support; **year**, year of sample date; **site**, accounted for possible non-independence of samples collected at the same site locality by including this random intercept effect; **active period length**, number of days between onset of spring and calling date; **active period mean temperature**, mean daily air temperature (˚C) throughout active period; **breeding period mean temperature**, mean daily air temperature (˚C) throughout breeding period; **active period mean precipitation**, mean precipitation (mm) throughout active period; **breeding period mean precipitation**, mean precipitation (mm) throughout breeding period; **hydroshed area** (km^2); **river density**, within 10 km buffer from site centroid; **road density**, within 50 km buffer from site centroid.

Model	Model description	*k*	logLik	AIC	ΔAIC	W_i	Retained
m8	factor(year) + river density * breeding period mean precipitation + hydroshed area + (1 | site)	9	-132.27	282.53	0.000	0.210	✓
m24	factor(year) + hydroshed area + (1 | site)	6	-135.27	282.53	0.000	0.210	✓
m28	factor(year) + breeding period mean temperature + hydroshed area + (1 | site)	7	-135.03	284.06	1.530	0.098	✗
m3	factor(year) + active period mean temperature + hydroshed area + (1 | site)	7	-135.16	284.32	1.792	0.086	✗
m12	factor(year) + breeding period mean precipitation + hydroshed area + (1 | site)	7	-135.20	284.40	1.870	0.082	✗
m6	factor(year) + active period mean precipitation + hydroshed area + (1 | site)	7	-135.21	284.41	1.880	0.082	✗
m9	factor(year) + river density + breeding period mean precipitation + hydroshed area + (1 | site)	8	-135.15	286.31	3.774	0.032	✗
m14	factor(year) + road density + breeding period mean precipitation + hydroshed area + (1 | site)	8	-135.16	286.33	3.796	0.031	✗
m25	factor(year) + (1 | site)	5	-138.47	286.94	4.404	0.023	✓
m10	factor(year) + river density * breeding period mean precipitation + (1 | site)	8	-135.94	287.88	5.348	0.014	✗
m13	factor(year) + road density * breeding period mean precipitation + hydroshed area + (1 | site)	9	-135.15	288.30	5.764	0.012	✗
m31	factor(year) + breeding period mean temperature + (1 | site)	6	-138.17	288.35	5.814	0.011	✗
m20	factor(year) + active period mean temperature + (1 | site)	6	-138.21	288.42	5.888	0.011	✗
m27	factor(year) + breeding period mean temperature + breeding period mean precipitation + (1 | site)	7	-137.24	288.49	5.954	0.011	✗
m19	factor(year) + breeding period mean precipitation + (1 | site)	6	-138.28	288.56	6.032	0.010	
m22	factor(year) + river density + (1 | site)	6	-138.36	288.71	6.182	0.010	
m21	factor(year) + active period mean precipitation + (1 | site)	6	-138.37	288.74	6.206	0.009	
m23	factor(year) + road density + (1 | site)	6	-138.38	288.75	6.220	0.009	
m29	factor(year) + breeding period mean temperature + river density + (1 | site)	7	-138.01	290.01	7.482	0.005	
m30	factor(year) + breeding period mean temperature + road density + (1 | site)	7	-138.04	290.08	7.550	0.005	
m18	factor(year) + active period mean temperature + road density + (1 | site)	7	-138.07	290.14	7.610	0.005	
m5	factor(year) + active period length * active period mean precipitation + (1 | site)	8	-137.14	290.28	7.752	0.004	
m4	factor(year) + active period mean temperature + river density + (1 | site)	7	-138.16	290.32	7.788	0.004	
m2	factor(year) + active period mean temperature + active period mean precipitation + (1 | site)	7	-138.19	290.38	7.850	0.004	
m1	factor(year) + active period length * active period mean temperature + (1 | site)	8	-137.21	290.41	7.878	0.004	
m11	factor(year) + river density + breeding period mean precipitation + (1 | site)	7	-138.21	290.43	7.896	0.004	
m16	factor(year) + road density + breeding period mean precipitation + (1 | site)	7	-138.23	290.47	7.934	0.004	
m7	factor(year) + active period mean precipitation + river density + (1 | site)	7	-138.31	290.62	8.088	0.004	
m17	factor(year) + active period mean precipitation + road density + (1 | site)	7	-138.33	290.66	8.130	0.004	
m15	factor(year) + road density * breeding period mean precipitation + (1 | site)	8	-138.12	292.24	9.706	0.002	
m26	1 + (1 | site)	3	-145.88	297.76	15.232	0.000	